AdS Black Holes from Localized Boundary Sources

João Pedro Alves da Silva
Mestrado em Física
Departamento de Física e Astronomia da Universidade do Porto
2015

Orientador
Miguel Sousa Costa, Professor Associado, Faculdade de Ciências da Universidade do Porto

Co-orientador
Jorge Eduardo Santos, Lecturer in Theoretical Physics, University of Cambridge

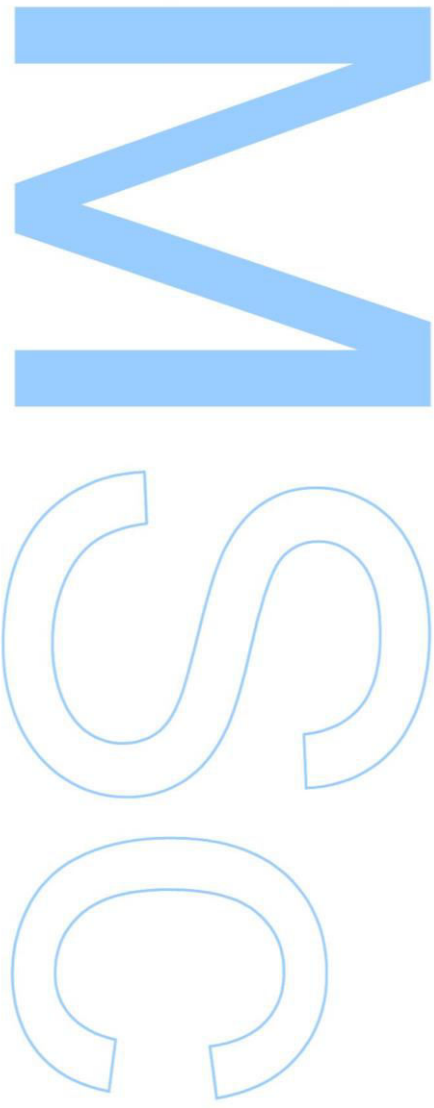

Todas as correções determinadas pelo júri, e só essas, foram efetuadas.

O Presidente do Júri,

Porto, _____/_____/_____

Acknowledgements

I'm very thankful for these 5 years in Porto, in particular for the past months where I've started to engage in research. I'd like to show my gratitude to Jorge Santos, for all his time and guidance. My time in Cambridge was very instructive. I'd also like to thank Miguel Costa for teaching me a lot of subjects. More generally, I'm grateful for all the friends and colleagues in FCUP.

I acknowledge the Gulbenkian Foundation for the significant financial support provided through *Programa de Estímulo à Investigação 2014*.

Abstract

We study a massive scalar field in a spacetime with a negative cosmological constant. We impose as boundary conditions that, near the conformal boundary, spacetime is AdS and the scalar field behaves as a localized defect. For the values of the field strength ϕ_B examined, we provide evidence that no Schwarzschild AdS black hole is formed. This is to be contrasted with the findings in *Hovering Black Holes from Charged Defects*, [Class. Quant. Grav., vol. 32, no. 10] by Horowitz, Iqbal, Santos and Way, where the authors considered an analogous setup, but with a maxwell field, instead of a scalar field. They found that, for a large class of profiles for the boundary maxwell field, a Reissner-Nördstrom AdS black hole is formed in the bulk.

In this thesis, we also review some topics involved in numerically solving the Einstein equations, namely the deTurck gauge and spectral methods in general relativity. We perform perturbative calculations as a check on our numerical work.

Resumo

Estudamos um campo escalar massivo, num espaço-tempo com constante cosmológica negativa. Impomos como condição de fronteira que, perto da fronteira conforme, o espaço-tempo é AdS e o campo escalar comporta-se como um defeito localizado. Para os valores do coeficiente do campo ϕ_B examinados, damos indícios de que nenhum buraco negro Schwarzschild AdS se forma. Isto deve ser contrastado com as investigações em *Hovering Black Holes from Charged Defects*, [Class. Quant. Grav., vol. 32, no. 10] por Horowitz, Iqbal, Santos e Way, em que os autores consideraram um cenário análogo, mas com um campo de maxwell, ao invés de um campo escalar. Eles obtiveram que, para uma vasta gama de tipos de campos de maxwell na fronteira, forma-se um buraco negro AdS Reissner-Nördstrom no interior do espao-tempo.

Nesta tese, também explicamos alguns tópicos envolvidos na resolução numérica das equações de Einstein, nomeadamente o calibre de deTurck e métodos espectrais em relatividade geral. Fazemos cálculos perturbativos de maneira a validar os nossos resultados numéricos.

Contents

List of Figures

1 Introduction

In [1], the authors solved the Einstein-Maxwell equations with a negative cosmological constant for a stationary and axisymetric spacetime, imposing that at the conformal boundary the metric is AdS and the maxwell field behaves as a localized source. The main finding was that, for a large class of profiles for the maxwell field on the boundary, if the source is *strong* enough, then a black hole is formed in the bulk. Moreover, for the profiles in which this happens, the size of the black hole increases universally as a function of the *strength* of the defect and does not depend on the particular way it decays. In this thesis, we study a similar scenario, but instead of a maxwell field we use a scalar field to serve as a localized defect.

In the first few sections, we review some well known topics. In section 2 we consider the deTurck gauge, which is essential for the numerical calculations involved in solving the Einstein equations. Afterwards, in section 3, we discuss the spectral method based on Chebyshev polynomials we used to solve our PDE's and we also explain our use of Newton's method. In section 4 we review the topics in gauge gravity duality that are relevant to our work. In section 5 we state the main results in [1] that motivated our work. In Appendix **C**, we define and prove a few properties about the Weyl tensor that we use. In Appendix **D**, we elaborate on the numerical hurdles we encountered. In Appendix **E**, we illustrate the powerful features of spectral methods in tackling general relativity calculations. Finally, in Appendix **F**, we display parts of our code.

The rest of the thesis contains original work. In section 6 we introduce our basic setup. We deal with the boundary conditions in section 7. This already involves some numerical work. In section 8 we display our numerical results for the bulk spacetime. Section 9 contains the conclusions and problems for the future. Appendix **A** and Appendix **B** contain the perturbative calculations we did as a check on our numerical results.

2 deTurck Gauge

2.1 General Remarks and Definition

A calculation in GR often involves writing an ansatz for the metric in terms of a few unknown fields and then using the Einstein equations and the matter field equations to solve for the unknown fields. The trouble is that it is often (but not always) the case that there are more unknowns than differential equations to solve for them. In this circumstance, the Einstein equations and the matter field equations by themselves are not enough to determine the metric.

Why does this happen? Generally, the metric can have $\frac{D(D+1)}{2}$ independent components. The Einstein equations involve the Ricci tensor, which is also a symmetric tensor. Yet, it has minus D independent components than the metric tensor, because of the Bianchi identities. Typically, the counting we have done is not accurate because when we write down an ansatz it doesn't have $\frac{D(D+1)}{2}$ independent components (the point of an ansatz is that it should only have a few). Despite this, this gives an idea why gauge redundancy happens.

Though the extra degrees of freedom contained in the metric are not physical, there's nothing wrong with them. They can be explained by the existence of diffeomorphism symmetry, to be explained in section 2.2. This corresponds to the fact that the ansatz does not totally fix the coordinate system we are in. This freedom in changing coordinate systems is the gauge freedom of general relativity.

Let us now define the deTurck vector. Consider a manifold equipped with a metric $g_{\mu\nu}$ and a background metric $\bar{g}_{\mu\nu}$. We want the background metric to be *near* the actual metric $g_{\mu\nu}$. The deTurck vector ξ^μ is defined as

$$\xi^\mu = g^{\alpha\beta}(\Gamma^\mu_{\alpha\beta}(g) - \Gamma^\mu_{\alpha\beta}(\bar{g}), \tag{1}$$

where the Γ's represent Christoffel symbols. The first is calculated for the actual metric and the second for the background metric. Notice that ξ^μ is a tensor, because the difference of Christoffel symbols is a tensor. Introducting the deTurck gauge consists in setting the deTurck vector equal to zero.

In order to motivate the definition of the deTurck vector, let us examine the possible character of the Einstein equations. As is well known, they constitute

a set of second order PDE's. Let us consider a general second order PDE in the variables x_1, ..., x_n. It can always be written in the form

$$\sum_{ij} L_{ij}(x_1, ..., x_n)\partial_i\partial_j u + ... = 0, \tag{2}$$

where ... means terms which do not involve second derivatives. This is reminiscent of the equations for the conic sections, with ∂_i replaced by x_i and L_{ij} constant. Just like for the conic sections, the behaviour of PDE's depends on the eigenvalues of the operator $L = \sum_{ij} L_{ij}(x_1, ..., x_n)\partial_i\partial_j$. Three cases are relevant for us

- All eigenvalues of L have the same sign (positive or negative). In this case, the PDE is called elliptic. The prototype for elliptic PDE's is the Laplace equation. In particular, the solutions are all analytic in the interior of their domain. They are usually solved by a relaxation method, which involves experimenting with some *guess* solution for the whole domain and then using an algorithm that, given the *guess*, improves on it to give a more accurate solution.

- One eigenvalue is negative and the others are all positive or one eigenvalue is positive and the others are all negative. In this case, the PDE is said to be hyperbolic. The prototype for this is the scalar wave equation. As opposed to elliptic equations, solutions to hyperbolic equations do not have to be smooth. Usually, the boundary conditions contain information about just one time slice and one solves the equation by evolving from one time slice to another. If the boundary conditions are non smooth, this is propagated in the solution for later times.

- One eigenvalue is 0 and the other ones are all positive or all negative. In this case, the PDE is called parabolic. The prototype for this is the heat equation. It is a hybrid between elliptic and hyperbolic equations.

The use of the deTurck gauge turns the Einstein equations into elliptic equations for stationary spacetimes. In subsection 2.3 we will give evidence as to why this is true. See [2] for more detailed explanations.

2.2 Diffeomorphisms

In this section, we just want to show why, given a certain vector A^μ, the metrics $g_{\mu\nu}$ and $g_{\mu\nu} + \epsilon\nabla_{(\mu}A_{\nu)}$, where ϵ is a very small quantity, are physically equivalent, in the sense that one can be obtained from the other by a coordinate transformation. This is a fact we will use in section 2.3

Consider a general spacetime equipped with a vector field V. Let us consider the set of curves $\{\gamma_i\}$ generated by V, i.e. such that at each point the velocity vector of these curves equals V at that point. It is clear that, if V is sufficiently smooth, these curves cover the whole of spacetime and do not intersect each other. Conversely, a set of curves with the last two preceding properties generates a smooth vector field V by the property of their velocities. From here, we conclude that the existence of a smooth vector field V is equivalent to the existence of a one parameter group of diffeomorphisms of spacetime on itself (the parameter is the parameter of the curves).

Let us consider a system of coordinates S, which labels a point P of spacetime by X^μ and which writes the metric in that point as $g_{\mu\nu}(X)$. Consider now a different coordinate system S', which labels the same point P of spacetime by $X'^\mu = X^\mu - V^\mu\epsilon$ and writes the metric at that point as $g'_{\mu\nu}(X')$. S' just labels the points differently from S by looking at the curves γ_i and lagging the time a little bit by ϵ.

We now wish to compare $g_{\mu\nu}(X)$ and $g'_{\mu\nu}(X)$. Note that this compares two different points of spacetime, yet the label X labels one point in S and the same label X labels another point in S'. We have that

$$g_{\mu\nu}(X) = \frac{\partial x'^\alpha}{\partial x^\mu}\frac{\partial x'^\beta}{\partial x^\nu}g'_{\alpha\beta}(X'). \tag{3}$$

Now note that

$$\frac{\partial x'^\alpha}{\partial x^\mu} = \delta^\alpha_\mu - \partial_\mu V^\alpha\epsilon + O(\epsilon^2), \tag{4}$$

$$g'_{\alpha\beta}(X') = g'_{\alpha\beta}(X) - \partial_\rho g'_{\alpha\beta}(X)V^\rho\epsilon + O(\epsilon^2). \tag{5}$$

Plugging the last two equations into (3) one obtains

$$g'_{\mu\nu}(X) = g_{\mu\nu}(X) + (\nabla'_\mu V_\nu + \nabla'_\nu V_\mu)\epsilon. \tag{6}$$

The lesson here is the following. Sometimes, one uses a certain label X for a point and writes a metric $g_{\mu\nu}$ on it. Afterwards, one decides to write another metric $g'_{\mu\nu}$ using the same label X. Yet, despite using the same label all the time, one has performed *a change of coordinates* (without noticing!).

2.3 Implementing the deTurck gauge

In order to investigate the character of the Einstein equations, let us look at the Ricci tensor $R_{\mu\nu}$ calculated from a metric $g_{\mu\nu}$ and perturb it with $g_{\mu\nu} \to g_{\mu\nu} + h_{\mu\nu}$, where $h_{\mu\nu}$ is a tiny perturbation with very small wavelength. For concreteness, we can put $h_{\mu\nu} = a_{\mu\nu} \exp(ik \cdot x)$, where $a_{\mu\nu}$ is tiny and k is very large. Since k is very large, when we examine $\delta R_{\mu\nu}$, we can assume $g_{\mu\nu}$ to be constant. To first order in $h_{\mu\nu}$, it is straightforward to obtain

$$\delta R_{\alpha\beta} = -\frac{1}{2}\Box h_{\alpha\beta} - \frac{1}{2}\partial_\alpha\partial_\beta h + \partial_\rho\partial_{(\alpha}h^\rho_{\beta)}, \tag{7}$$

where $\Box \equiv g^{\mu\nu}\partial_\mu\partial_\nu$. Looking at equation 7, it is clear that we can find some nonzero value of k for which $\delta R_{\mu\nu}$ is null. This isn't surprising, as we know that the Einstein equations can have a wavelike character. We will now make certain assumptions, so as to eliminate this possibility.

To deal with this problem, first notice that we are only considering stationary spacetimes, so $\Box \to \nabla^2$. The pernicious

$$-\frac{1}{2}\partial_\alpha\partial_\beta h + \partial_\rho\partial_{(\alpha}h^\rho_{\beta)}. \tag{8}$$

term will be dealt with by the deTurck gauge.

It is intructive to notice that $\delta R_{\mu\nu}$ is insensitive to the change in the perturbation $h_{\mu\nu} \to h_{\mu\nu} + \nabla_\mu w_\nu$, where $w_{\mu\nu}$ is a tiny vector field. This corresponds to the usual diffeomorphism freedom explained in section 2.2.

We would like to define a quantity dependent on the metric such that its change with $g_{\mu\nu} \to g_{\mu\nu} + h_{\mu\nu}$ is equal to (8). The gauge condition would then consist in fixing this quantity. Consider

$$g^{\lambda\nu}(\partial_\lambda g_{\nu\mu} - \frac{1}{2}\partial_\mu g_{\lambda\nu}). \tag{9}$$

Its change with $g_{\mu\nu} \to g_{\mu\nu} + h_{\mu\nu}$ is

$$\frac{1}{2}\partial_\mu h + \partial_\lambda h^\lambda_\mu. \tag{10}$$

If this is zero, then (8) is null, just like we wanted. The deTurck vector is nothing but a covariant version of (9).

Using the fact that the covariant derivative of the metric is zero (using the Christoffel symbols), one obtains that the upper index version of (9) is equal to

$$g^{\alpha\beta}\Gamma^\rho_{\alpha\beta}. \tag{11}$$

This is a non covariant quantity. We can make it covariant by instead considering

$$\xi^\rho = g^{\alpha\beta}(\Gamma^\rho_{\alpha\beta} - \bar{\Gamma}^\rho_{\alpha\beta}), \tag{12}$$

where $\bar{\Gamma}^\rho_{\alpha\beta}$ is the Christoffel symbol calculated with respect to a fixed background metric. This is a covariant quantity, because the difference of Christoffel symbols is a tensor. It is called the deTurck vector. Finally, notice it has the same transformation properties with respect to $g_{\mu\nu} \to g_{\mu\nu} + h_{\mu\nu}$ that (11) has.

How to implement the deTurck gauge? We will take advantage of the following fact. Under the transformation $g_{\mu\nu} \to g_{\mu\nu} + h_{\mu\nu}$, the change in $\nabla_{(\mu}\xi_{\nu)}$ is equal to (8). So, the operator

$$R^H_{\mu\nu} = R_{\mu\nu} - \nabla_{(\mu}\xi_{\nu)}, \tag{13}$$

is elliptic. This means that when using the deTurck gauge we should always replace $R_{\mu\nu} \to R^H_{\mu\nu}$. In substitution of the Einstein equations, we call the corresponding equations Einstein-deTurck.

In practice, instead of simultaneously solving the Einstein-deTurck equations and the gauge equation $\xi^\mu = 0$, we will just solve the Einstein-deTurck equations and hope that in the end the deTurck vector ends up being zero. In all our numerical calculations, we have checked that this is so[1]. Under certain assumptions, it is possible to prove that there are no solutions to the Einstein-deTurck equations with nonzero ξ^μ. When such solutions exist, they are called Ricci solitons. See [3] for more details.

[1] In all our numerical calculations, we made sure $\xi^\mu\xi_\mu < 10^{-10}L^{-2}$, where L is the AdS length.

3 Chebyshev Polynomials and Newton's method

We now explain how we numerically solved the Einstein-deTurck equations.

3.1 Chebyshev Polynomials

[2]Chebyshev polynomials are a complete basis for smooth functions defined on $[-1,1]$. Given a function $f(x)$, we define its Nth order Chebyshev interpolant as $\sum_{n=0}^{N} a_n T_n(x)$, where $T_n(x)$ is the nth order Chebyshev polynomial and a_n is a coefficient which depends on the function f. In the limit $N \to \infty$ the Chebyshev interpolant will converge to f, if f is sufficiently smooth. In this section, we will define the Chebyshev polynomials and show how to compute the Chebyshev interpolant (i.e., the coefficients a_n) of a smooth function defined on a bounded interval.

Suppose we have a function $f(x)$ defined on a bounded interval $[a,b]$ which we want to approximate using an Nth order interpolant. We can rescale this interval to $[-1,1]$, approximate the function in this new domain using Chebyshev polynomials and then rescale back again to the original domain. Thus, without loss of generality, we will always assume that functions in this section are defined on $[-1,1]$ (if a function is 2d, we will say the domain is $[-1,1]\times[-1,1]$, etc).

Let us look at the interval $[-1,1]$ in the complex plane.

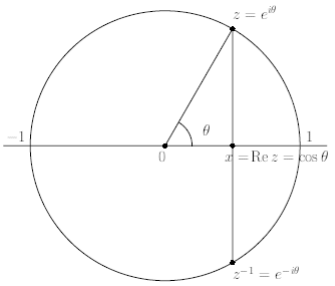

Figure 1: Suppose we want to approximate a function $f(x)$, where $x \in [-1,1]$. Putting $\theta \equiv \arccos(x)$, let us define $g : [-\pi,\pi] \to \mathcal{R}$ such that $g(\theta) = f(x)$ for $-\pi \le \theta \le 0$ and $g(\theta)$ is even.

[2]We follow [4] here.

Since $g(-\pi) = g(\pi)$, g can easily be extended to a periodic function of period 2π. Thus, it is possible to write $g(\theta)$ as a Fourier series: $g(\theta) = \sum_{n=0}^{+\infty} a_n \cos(n\theta)$ (the series only involves $\cos$ because g is even). We can now define an Nth order trigonometric interpolant of g as $Q_N \equiv \sum_{n=0}^{N} a_n \cos(n\theta)$. From this, we obtain an interpolant $P_N(x)$ of $f(x)$ by defining $P_N(x) = Q_N(\theta)$, where x and θ are related by $x = \cos(\theta)$. Thus, $P_N(x) = \sum_{n=0}^{N} a_n \cos(n \arccos x)$. It is easy to check that $\cos(n \arccos x)$ is polynomial in x. We thus define $T_n(x) \equiv \cos(n \arccos x)$. The coefficients a_n can be computed by usual Fourier analysis methods in $g(\theta)$. This estabilishes an intimate connection between expansion in Chebyshev polynomials for functions defined on $[-1, 1]$ and Fourier expansion for functions defined on $[-\pi, \pi]$.

We must now decide which interpolating points to use in the $[-1, 1]$ domain. We have seen that interpolating $f(x)$ by $P_N(x)$ is equivalent to interpolating $g(\theta)$ with $Q_N(\theta)$. For the domain $[-\pi, \pi]$ it is natural to choose the interpolating points $\theta_n = n\frac{\pi}{N}$, with $n = -N + 1, ..., N$. In condensed matter physics language, these points constitute the first Brillouin zone. We are thus led to the definition of Chebyshev nodes $x_n = \cos(n\frac{\pi}{N})$, $n = 0, ..., N$ which we will use as interpolating points. Notice that the Chebyshev nodes are distributed throughout the entire $[-1, 1]$ region, with particular emphasis on the borders. Because of this, we say that Chebyshev interpolation is a global interpolation method, since it takes into account a function's behaviour in its entire domain and not just on a single region.[3]

3.2 Newton's method

We will now give the final step involved in solving the Einstein equations numerically. For simplicity, we will assume we are dealing with just one ODE, instead of with a set of PDE's, but the generalisation will be trivial.

Consider then an ODE in a certain unknown function $q(x)$ and suppose we have already picked the nodes x_0, ..., x_N we want to use. Using the nodes, we turn the ODE into a set of $N + 1$ system of equations. To each inner node,

[3] The previous motivation for the Chebyshev polynomials is neat, but it doesn't explain why they work so well. In fact, the most important property of the Chebyshev polynomials is that, for large number N of nodes, its nodes have a density of $\frac{N}{\pi\sqrt{1-x^2}}$. (See [4] for the details.)

will correspond an equation that can be obtained from the ODE by making substitutions of the sort $q(x) \to q_i$, $q'(x) \to q'_i$, $q''(x) \to q''_i$, where q_i, q'_i, ... are new unkowns. q_i represents the value of q at the node i, q'_i represents the value of the derivative at the node i, etc. For example, suppose the ODE is $q''(x) + q(x)^2 = 0$. Then, we will have a system of equations $q''_i + q_i^2 = 0$, $i = 1$,..., $N - 1$. For the outer nodes, we impose boundary conditions. For example, if $q(x) = 0$ at $x = x_0$, then we add the equation $q_0 = 0$.

This procedure generates $N + 1$ equations for more than $N + 1$ unknowns, because each value of the function q at the nodes is an unknown, each derivative is another unknown, each second derivative is another unknown, etc. Let us now relate the derivatives q'_i, q''_i, ..., with the values q_i. Suppose we pick as nodes the Chebyshev nodes. We can write a polynomial interpolation of q as

$$q(x) = \sum_{i=0}^{i=N} q_i P_i^N(x), \tag{14}$$

where $P_i^N(x)$ is a polynomial of degree N which is zero at $x_0, ..., x_{i-1}, x_{i+1}, ..., x_N$ and 1 at x_i. So

$$q'_i = \sum_{j=0}^{j=N} D_{ij} q_j, \tag{15}$$

where $D_{ij} = P_j^{'N}(x_i)$. This generalizes to second derivatives and so on. The differentiation matrix D_{ij} only has to be obtained once for the entire calculation. See [4] for formulae.

The preceding procedure turns an ODE into a system of $N + 1$ equations in the unknowns q_0, ..., q_N. We do not start to solve this immediately, because this system is often not linear. We deal with this using Newton's method. First, let us view the previous system of equations as an equality of the sort $f_i(q) = 0$, where $q = (q_0, ..., q_N) \in \Re^{N+1}$ and f is a function $\Re^{N+1} \to \Re^{N+1}$. Suppose now we have a guess q_{guess} for the previous equality[4]. We linearize $f_i(q) = f_i(q_{guess}) + \frac{\partial f_i}{\partial q_j}(q_j - (q_j)_{guess})$, where the matrix $\frac{\partial f_i}{\partial q_j}$ is calculated at q_{guess}. We have now a linear system of equations

[4] In this particular work, suppose we are solving for the metric at low Φ. Then, we can use as q_{guess} the information we already know about the AdS metric. For higher ϕ_B, say we know the metric for $\phi_B = 1.0$, we can use that as q_{guess} for the metric at $\phi_B = 1.1$ and so on.

$$A(q_{guess})_{ij}\Delta q_j = B(q_{guess})_j, \tag{16}$$

where $A(q_{guess})_{ij} = \frac{\partial f_i}{\partial q_j}$ and $B(q_{guess})_j = -f(q_{guess})_j$. Next we use a standard linear solver to obtain Δq and improve our guess $q_{guess} \to q_{guess} + \Delta q$. We do this repeatedly until our successive guesses always become the same. Notice that, for this method to work, it is important that the initial guess is close enough to the actual solution.

4 Gauge Gravity Duality

4.1 Anti-deSitter Space

Let us consider the vacuum Einstein equations with a cosmological constant Λ,

$$R_{\mu\nu} - \frac{1}{2}Rg_{\mu\nu} + \Lambda g_{\mu\nu} = 0. \tag{17}$$

Contracting, one finds that $R = \frac{2d}{d-2}\Lambda$. Thus, R is a constant. Also, by manipulating (17), we obtain that the Ricci tensor has the form $R_{\mu\nu} = \frac{R}{d}g_{\mu\nu}$. Still, this does not fix the spacetime we're in, because there are many physically distinguishable metrics which satisfy (17) for a certain Λ.

In Appendix **C**, we show that knowing the Ricci tensor does not exhaust the degrees of freedom contained in the Riemann tensor. The extra degrees of freedom are contained in an object called the Weyl tensor. Let us consider spacetimes with a cosmological constant (i.e. (17) is satisfied) with zero Weyl tensor. The Riemann tensor then takes the simple form

$$R_{abcd} = \frac{R}{d(d-1)}(g_{ac}g_{bd} - g_{ad}g_{bc}). \tag{18}$$

Manifolds that satisfy (18) are called *constant curvature spacetimes*. Notice that, by virtue of the Bianchi identities, (18) by itself implies that the curvature is constant, without there being any need to invoke Einstein's equations.

There is a theorem (see [5]) which says that constant curvature spacetimes with the same curvature, dimension and metric signature are locally isometric. Thus, to classify constant curvature spacetimes, all we need to do is find examples with every value of R. If the signature is Euclidean, there are three

possible cases. If $R > 0$, the geometry is spherical; if $R = 0$, spacetime is flat; if $R < 0$, we have an hyperboloid. If the signature is Lorentzian, then if $R > 0$ we find deSitter space, $R = 0$ is flat space and $R < 0$ is Anti-deSitter space.

We now show how to parameterize euclidean constant curvature spacetimes. This is instructive, as the parameterizations of deSitter and anti-deSitter space that we will show next will look more natural. We start with a d-sphere embedded in d+1 dimensional euclidean spacetime,

$$(z_1)^2 + ... + (z_{d+1})^2 = L^2. \tag{19}$$

We use coordinates

$$\begin{aligned} z_1 &= L\cos(\theta_1), \\ z_2 &= L\sin(\theta_1)\cos(\theta_2), \\ &... \\ z_d &= L\sin(\theta_1)...\cos(\theta_d), \\ z_{d+1} &= L\sin(\theta_1)...\sin(\theta_d). \end{aligned} \tag{20}$$

We can now plug this into the euclidean metric $dz_1^2 + ... + dz_{d+1}^2$ to get the induced metric on the d-sphere,

$$ds^2 = L^2(d\theta_1^2 + \sin^2(\theta_1)(d\theta_2^2 + \sin^2(\theta_2)(...\sin^2(\theta_{d-1})d\theta_d^2)...). \tag{21}$$

Using this metric, we can now calculate the Riemann tensor (say, using Mathematica) and see that indeed it has the form of (18).

The d dimensional euclidean $R < 0$ constant curvature spacetime can be obtained by the embedding

$$-(z_1)^2 + ... + (z_{d+1})^2 = -L^2 \tag{22}$$

in $\mathbb{R}^{1,d}$, where $\mathbb{R}^{1,d}$ is a $d+1$ dimensional spacetime with metric $-(dz_1)^2 + ... + dz_{d+1}^2$, i.e. it has one time coordinate and d space coordinates. To parameterize, by comparison with (20), we need to have hyperbolic sines and hyperbolic

cosines, to get the required minus signs in (22). So, we put

$$\begin{aligned} z_1 &= L\cosh(\Psi), \\ z_2 &= L\sinh(\Psi)\cos(\theta_2), \\ &... \\ z_d &= L\sinh(\Psi)...\cos(\theta_d), \\ z_{d+1} &= L\sinh(\Psi)...\sin(\theta_d), \end{aligned} \tag{23}$$

where $\Psi \in [0, +\infty]$. The induced metric is $L^2 d\Psi^2 + L^2 \sinh^2(\Psi) d\Omega_{d-1}^2$.

Let us consider now Lorentzian constant curvature spacetimes. The $R > 0$ case is just the analogue of (19), yet we are embedding in $\mathbb{R}^{(1,d)}$ and not in $\mathbb{R}^{(0,d+1)}$ like in (19),

$$-(z_1)^2 + ... + (z_{d+1})^2 = L^2. \tag{24}$$

The parameterization is

$$\begin{aligned} z_1 &= L\sinh(\Psi), \\ z_2 &= L\cosh(\Psi)\cos(\theta_2), \\ &... \\ z_d &= L\cosh(\Psi)...\cos(\theta_d), \\ z_{d+1} &= L\cosh(\Psi)...\sin(\theta_d). \end{aligned} \tag{25}$$

The induced metric (which is the deSitter metric) is

$$ds^2 = -L^2 d\Psi^2 + L^2 \cosh^2(\Psi) d\Omega_{d-1}^2. \tag{26}$$

Finally, we consider the $R < 0$ case with Lorentzian signature, that is, the AdS metric. It is the analogue of (22), but we are embedding in $\mathbb{R}^{(2,d-1)}$ and not in $\mathbb{R}^{(1,d)}$, like in (22),

$$-(z_1)^2 - (z_2)^2 + (z_3)^2 + ... + (z_{d+1})^2 = -L^2. \tag{27}$$

The line element of $\mathbb{R}^{(2,d-1)}$ is $-(dz_1)^2 - (dz_2)^2 + (dz_3)^2 + ... + (dz_{d+1})^2$. The

parameterization is

$$\begin{aligned} z_1 &= L\cosh(\Psi)\cos(\theta_2), \\ z_2 &= L\cosh(\Psi)\sin(\theta_2), \\ z_3 &= L\sinh(\Psi)\cos(\theta_3), \\ z_4 &= L\sinh(\Psi)\sin(\theta_3)\cos(\theta_4), \\ &\dots \\ z_d &= L\sinh(\Psi)...\cos(\theta_d), \\ z_{d+1} &= L\sinh(\Psi)...\sin(\theta_d). \end{aligned} \tag{28}$$

The induced metric is the AdS metric, which is

$$ds^2 = -L^2\cosh^2(\Psi)d\theta_2^2 + L^2 d\Psi^2 + L^2\sinh^2(\Psi)d\Omega_{d-2}^2. \tag{29}$$

Notice $\theta_2 \in [-\pi, \pi]$ is a time coordinate[5].

We will now try to understand AdS space from the point of view of symmetry. We start by introducing a few relevant concepts. A maximally symmetric spacetime is a spacetime with the maximum allowed number of linearly independent Killing vector fields. A d dimensional spacetime can have only $\frac{d(d+1)}{2}$ independent Killing vector fields, a fact we will now prove.

We start by deriving the formula

$$\nabla_a\nabla_b\xi_c = -R^d_{bca}\xi_d, \tag{30}$$

where ξ^μ is a Killing vector field. We have that

$$\nabla_a\nabla_b\xi_c - \nabla_b\nabla_a\xi_c = R^d_{abc}\xi_d, \tag{31}$$

$$\nabla_c\nabla_a\xi_b - \nabla_a\nabla_c\xi_b = R^d_{cab}\xi_d, \tag{32}$$

$$\nabla_b\nabla_c\xi_a - \nabla_c\nabla_b\xi_a = R^d_{bca}\xi_d. \tag{33}$$

Using Killing's equation,

$$\nabla_a\nabla_b\xi_c - \nabla_b\nabla_a\xi_c = R^d_{abc}\xi_d, \tag{34}$$

$$\nabla_c\nabla_a\xi_b + \nabla_a\nabla_b\xi_c = R^d_{cab}\xi_d, \tag{35}$$

$$-\nabla_b\nabla_a\xi_c + \nabla_c\nabla_a\xi_b = R^d_{bca}\xi_d. \tag{36}$$

[5]We can extend this coordinate to $\mathbb{R}$. In this case, we get infinite copies of AdS_d.

Now consider (34)+(35)-(36) and use the Bianchi identities to get (30).

We will now use (30) to show that if we know ξ_μ and $L_{\mu\nu} \equiv \nabla_\mu \xi_\nu$ at any point P of spacetime, then we know ξ_μ and $L_{\mu\nu}$ everywhere. Consider then a point P of spacetime where ξ_μ and $L_{\mu\nu}$ are known and consider another arbitrary point Q of spacetime. Let V^μ be a vector field, such that it generates a curve γ that goes from P to Q. To know how ξ_μ and $L_{\mu\nu}$ change along γ, we can solve a set of ODE's,

$$\begin{aligned} V^\mu \nabla_\mu \xi_\nu &= V^\mu L_{\mu\nu}, \\ V^\mu \nabla_\mu L_{\alpha\beta} &= -V^\mu R^\nu_{\alpha\beta\mu} \xi_\nu. \end{aligned} \tag{37}$$

This is first order, so knowing ξ_μ and $L_{\mu\nu}$ at P are enough initial conditions to solve it. Thus, the values of ξ_μ and $L_{\mu\nu}$ at Q are completely fixed by their values at P.

We now investigate the number of independent components of ξ_μ and $L_{\mu\nu}$ at P. ξ_μ has d independent components and $L_{\mu\nu}$ has $\frac{d(d-1)}{2}$, because of Killing's equation. So, there are at most $\frac{d(d-1)}{2} + d = \frac{d(d+1)}{2}$ linearly independent Killing vector fields.

As an example of maximally symmetric spaces, consider a d dimensional homogeneous and isotropic euclidean spacetime. Homogeneity means that there is an isometry between any two points of spacetime. Isotropy means that, for every point P of spacetime, if you take two arbitrary vectors V^μ and W^μ belonging to the tangent space at P, then there's an isometry which leaves P fixed and transforms V^μ into W^μ. There are d Killing vector fields which generate translations (homogeneity) and $\frac{d(d-1)}{2}$ Killing vectors fields which generate rotations (isotropy), so we conclude that euclidean homogeneous and isotropic spacetime is maximally symmetric.

Continuing this example, we will now show how the properties of homogeneity and isotropy imply that spacetime is of constant curvature, i.e. (18) holds. Consider the Riemann tensor with two indices down and two up R^{cd}_{ab}. By virtue of its symmetries, we can view the Riemann tensor as a linear operator L from the space W of antissymetric tensors of rank $(0,2)$ on itself. W has an inner product generated by the metric, i.e. given any two elements w_{ab} and v_{ab} of W, we define their inner product as $w_{ab}v^{ab}$. Notice that this inner

product is positive definite, since the signature of the metric is euclidean. Since $R_{abcd} = R_{cdab}$, the operator L is self adjoint with respect to this inner product. Thus, W has a basis composed of a set of linearly independent eigenvectors of L. Now, because of isotropy, no two eigenvectors can be distinguished from each other and so all the eigenvalues are the same. This means that L must be equal to KI, where K is the eigenvalue and I is the identity operator. Because of translation symmetry, K is the same everywhere. In terms of components, this implies that

$$R^{cd}_{ab} = K\delta^{[c}_{[a}\delta^{d]}_{b]}. \tag{38}$$

Lowering the indices, we arrive at equation (18), with $K = \frac{R}{d(d-1)}$.

Let us now show that constant curvature spacetimes are maximally symmetric. For example, consider AdS_d. As we have seen, it can be viewed as the surface

$$-(z_1)^2 - (z_2)^2 + (z_3)^2 + ... + (z_{d+1})^2 = -L^2 \tag{39}$$

in $\mathbb{R}^{2,d-1}$. $\mathbb{R}^{2,d-1}$ is a $d+1$ dimensional maximally symmetric space, with translational and rotational symmetry. When we pass to AdS_d, we lose all translations, but we keep all rotations. The group of rotations of $\mathbb{R}^{2,d-1}$ is $SO(2, d-1)$, which has $\frac{(d+1)d}{2}$ generators. Thus, AdS_d is maximally symmetric. An analogous argument works for the other constant curvature spacetimes.

We turn our attention to the causal structure of Anti-deSitter space. It is useful to change coordinates and draw a diagram. Before doing that, we start by drawing the Penrose diagram of Minkowski space, as it will be useful to compare. The point of Penrose diagrams is to write coordinates where infinities can be brought to finite values of the coordinates. Instead of using the metric $g_{\mu\nu}$ of the system we are looking to study, we consider instead a metric $\Omega^2 g_{\mu\nu}$ conformal to the first one. This preserves the causal structure of spacetime, which is what we are interested in. This can be made clear by an example.

Consider then two dimensional Minkowski space with metric $ds^2 = -dt^2 + dx^2$. Define now $u = \frac{-t+x}{2}$ and $v = \frac{t+x}{2}$. With these definitions, the metric becomes $ds^2 = -dudv$. Define now $\tilde{U}$ and $\tilde{V}$ by $\tan(\tilde{U}) = u$ and $\tan(\tilde{V}) = v$. Notice that both $\tilde{U}$ and $\tilde{V}$ range from $-\frac{\pi}{2}$ to $\frac{\pi}{2}$. In that case, we obtain that

$ds^2 = \frac{1}{\cos(\tilde{U})^2 \cos(\tilde{V})^2}(-d\tilde{U}d\tilde{U})$. Defining now $\tilde{T} = \tilde{V} - \tilde{U}$ and $\tilde{X} = \tilde{U} + \tilde{V}$ we get

$$ds^2 = \frac{-d\tilde{T}^2 + d\tilde{X}^2}{4\cos(\frac{-\tilde{T}+\tilde{X}}{2}\cos(\frac{\tilde{T}+\tilde{X}}{2})}. \tag{40}$$

Geometrically, this can be represented by a diagram:

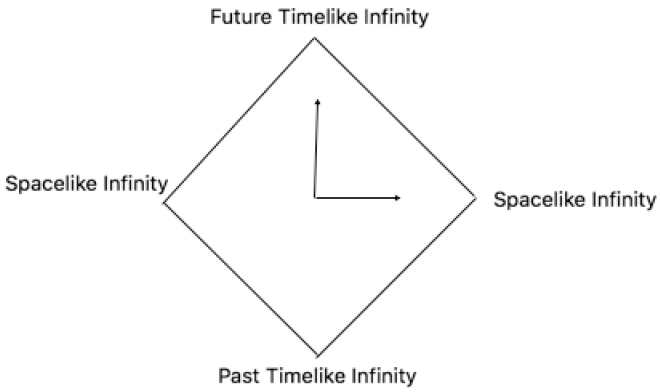

Figure 2: Penrose diagram of Minkowski space. The vertical coordinate represents $\tilde{T}$ and the horizontal coordinate $\tilde{X}$. The tilted lines represent lightlike infinity. $\tilde{T}$ and $\tilde{X}$ range from $[-\pi, \pi]$.

Let us now turn our attention to Anti-deSitter space. Consider the AdS_d metric $ds^2 = -L^2\cosh^2(\Psi)d\tau^2 + L^2 d\Psi^2 + L^2\sinh^2(\Psi)d\Omega^2_{d-2}$, where we have extended already $\tau \in \mathbb{R}$. Consider the change of coordinates $\tan(\theta) = \sinh(\psi)$, where $\theta \in [0, \frac{\pi}{2}]$, because $\psi \in [0, +\infty]$. The line element is now $ds^2 = \frac{1}{\cos^2(\theta)}(-d\tau^2 + d\theta^2 + \sin^2(\theta)d\Omega^2_{d-2})$. This is not quite a Penrose compactification, since we were unable to bring infinities in τ to finite values (see figure (3)).

Finally, we introduce a new set of coordinates of Anti-deSitter space, called Poincaré coordinates. As we have seen already, we can view AdS_d as the following surface in $\mathbb{R}^{2,d-1}$,

$$-(z_1)^2 + (-z_2 + z_3)(z_2 + z_3) + \sum_{i=4}^{d+1} z_i^2 = -L^2. \tag{41}$$

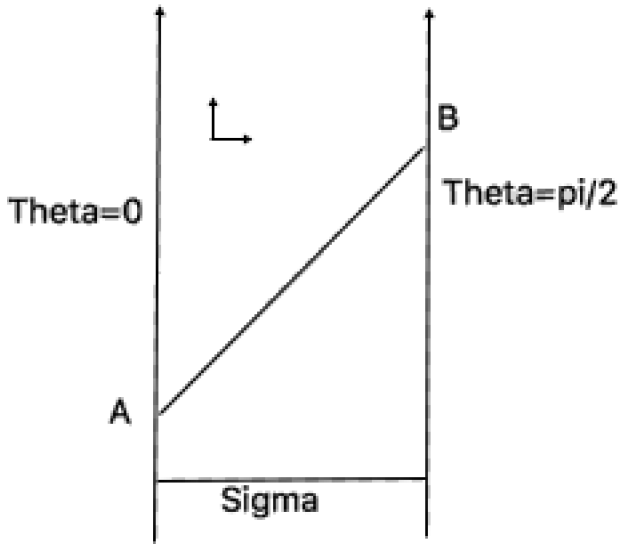

Figure 3: Diagram of AdS space. The vertical coordinate represents τ and the horizontal coordinate θ. Notice that $\theta \in [0, \frac{\pi}{2}]$, while $\tau \in \mathbb{R}$. Σ is a spacelike surface and the line that goes from point A to point B represents the path of a light ray. If we place observers at every point of Σ, they will be ignorant of the light ray just described, because it does not cross Σ. Hence, Σ is not a Cauchy surface. AdS has no Cauchy surfaces, since, if you draw a spacelike surface, you can always find light rays that travel from lightlike infinity to lightlike infinity without ever crossing that spacelike surface, as this drawing illustrates.

Consider the coordinates,

$$\begin{aligned} z_1 &= t\exp(\frac{y}{L}), \\ z_2 &= L\cosh(\frac{y}{L}) + \frac{\exp(\frac{y}{L})}{2r}(x^2 - t^2), \\ z_3 &= L\sinh(\frac{y}{L}) - \frac{\exp(\frac{y}{L})}{2r}(x^2 - t^2), \\ z_{3+i} &= x_i \exp(\frac{y}{L}), \end{aligned} \tag{42}$$

with $i = 1, ..., d-2$ and $x^2 = \sum_{i=1}^{d-2} x_i^2$. By substituting (42) into the lhs of (41), we see that indeed we get $-L^2$. Yet, notice that we are only parameterizing half of AdS_d, because $z_2 + z_3 = L\exp(\frac{y}{L}) > 0$. The induced metric is obtained by putting (42) into the metric of $\mathbb{R}^{(2,d-1)}$. We get $ds^2 = \exp(\frac{2y}{L})(-dt^2 + dx^2) + dy^2$.

Finally, defining the z coordinate such that $\exp(\frac{y}{L}) = \frac{L}{z}$, we obtain

$$ds^2 = \frac{L^2}{z^2}(-dt^2 + dz^2 + dx^2), \tag{43}$$

where z goes from 0 to $+\infty$.

4.2 Anti-deSitter Black Holes

Anti-deSitter black holes are black hole solutions to the vacuum Einstein equations with a negative cosmological constant. Since our thesis problem is in 4 dimensions, we will restrict our discussion to that case. We start by rewriting the AdS_4 metric. Consider the metric as written in (29). Let us extend the domain of θ_2 to $\mathbb{R}$ and do the transformation $t = L\theta_2$ and $r = L\sinh(\Psi)$. We obtain

$$ds^2 = -(1 + \frac{r^2}{L^2})dt^2 + \frac{dr^2}{1 + \frac{r^2}{L^2}} + r^2 d\Omega_2^2. \tag{44}$$

(44) looks similar to the Schwarzschild metric. It turns out that, if we add a "Schwarzschild term" to this metric, then we obtain the metric

$$ds^2 = -(1 - \frac{2M}{r} + \frac{r^2}{L^2})dt^2 + \frac{dr^2}{1 - \frac{2M}{r} + \frac{r^2}{L^2}} + r^2 d\Omega_2^2, \tag{45}$$

which is still a solution to the vacuum Einstein equations with a negative cosmological constant. Notice that this metric contains a black hole, whose horizon is at r^*, where r^* is such that $1 - \frac{2M}{r^*} + \frac{(r^*)^2}{L^2} = 0$. We observe that, defining $g(r) \equiv 1 - \frac{2M}{r} + \frac{r^2}{L^2}$, then $g'(r) > 0$ always. Since $\lim_{r\to 0} g(r) = -\infty$ and $\lim_{r\to+\infty} g(r) = +\infty$, then $g(r)$ has a root and it is unique. A spacetime with the metric (45) is called AdS-Schwarzschild.

It is well known that stationary black holes exhibit thermodynamical behaviour, through the so called laws of black hole mechanics. In particular, a black hole's temperature T is equal to $\frac{k}{4\pi}$, where k is the surface gravity. We now show how to calculate the temperature of black holes with metrics of the type

$$ds^2 = -f(r)dt^2 + \frac{1}{f(r)}dr^2 + r^2 d\Omega_2^2, \tag{46}$$

where the function $f(r)$ is zero at the horizon. Our method is quick, yet heuristic[6]. An important result in quantum field theory at finite temperature is that

[6]There's a more rigorous argument that gives the same result, which involves using the definition of the surface gravity in terms of a Killing vector.

the partition function of a system at temperature T can be written as the path integral of a quantum field theory, where in the path integral we consider time to be an imaginary and periodic quantity with period $\frac{1}{T}$ (see [6]). Guided by that principle, we consider the euclidean version of (46), i.e. we picture time as an imaginary quantity $t = i\tau$, where τ is a real variable. Near the horizon r^*, $f(r) \sim f'(r^*)(r - r^*)$, so we define a coordinate ρ such that $d\rho^2 = \frac{dr^2}{f'(r^*)(r-r^*)}$. More explicitly, we define $\rho \equiv \sqrt{(r - r^*)}\frac{2}{\sqrt{f'(r^*)}}$. The metric is then

$$ds^2 = \frac{\rho^2 f'(r^*)^2}{4}d\tau^2 + d\rho^2 + r(\rho)^2 d\Omega_2^2. \tag{47}$$

As we mentioned before, τ should be periodic. When $\rho \to 0$, the $\frac{\rho^2 f'(r^*)^2}{4}d\tau^2 + d\rho^2$ portion of the metric should reduce to $\mathbb{R}^2$. Thus, τ must have period $\frac{4\pi}{f'(r^*)}$, so the temperature of the black hole is $\frac{f'(r^*)}{4\pi}$.

Let us now see some examples of this formula. For a Schwarzschild black hole, $f(r) = 1 - \frac{2M}{r}$, so $T = \frac{1}{8\pi M}$. For a Schwarzschild AdS black hole, after some algebraic manipulations, we get $T = \frac{L^2+3(r^*)^2}{4\pi L^2 r^*}$.

It is instructive to compare the specific heat of Schwarzschild and AdS-Schwarzschild black holes. For Schwarzschild, $\frac{\partial T}{\partial M} = -\frac{1}{8\pi M^2}$. This is negative, which means that Schwarzschild black holes are unstable thermodynamic objects. To see that, consider putting a Schwarzschild black hole at temperature T in contact with a heat bath at temperature T_0. If $T_0 > T$, the heat bath provides energy to the black hole. Since $\frac{\partial T}{\partial M} < 0$, this causes the temperature of the black hole to go down, so the system goes away from thermodynamic equilibrium. Analogously, if $T_0 < T$, the black hole loses energy, yet its temperature increases, so once again one deviates from thermodynamic equilibrium.

AdS-Schwarzschild black holes don't suffer from this disease. For them, $\frac{\partial T}{\partial M} = \frac{3(r^*)^2-L^2}{4\pi L^2 (r^*)^2}\frac{1}{M+\frac{(r^*)^3}{L^2}}$, so $\frac{\partial T}{\partial M}$ is positive if $r^* > \frac{L}{\sqrt{3}}$, which happens for $M > \frac{2}{3\sqrt{3}}L$.

4.3 Some comparisons between gravity in AdS and CFT's

[7] We start by comparing the degrees of freedom of a quantum field theory in d dimensional Minkowski space to a gravity theory in Anti-deSitter space in $d+1$ dimensions, using the holographic principle.

[7] We reference [7] here.

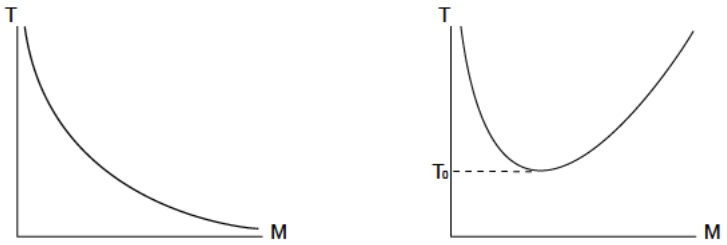

Figure 4: At the left, the graph refers to AdS_4 and at the right to AdS_4-Schwarzschild. The specific heat of AdS_4-Schwarzschild is positive after $M > \frac{2}{3\sqrt{3}}L$.

To simulate a quantum field theory, suppose we arrange a $d-1$ dimensional cubic lattice, with linear size R and separation between lattice points ϵ. The number of degrees of freedom of the quantum field theory are then $\frac{R^{(d-1)}}{\epsilon^{(d-1)}}N_s$, where N_s are the number of degrees of freedom per lattice site.

The holographic principle states that the degrees of freedom of a system are contained in its boundary. Specifically, for AdS_{d+1}, it says that the number of degrees of freedom are equal to $\frac{A}{4G_N}$, where A is the area of the conformal boundary and G_N is Newton's constant, which has dimensions of $[Length]^{d-1}$ in units where $c = 1$ and $\hbar = 1$. A is equal to $\int_{z=0;t=t_0} d^{d-1}x\sqrt{g}$. Now, in this case, $\sqrt{g} = \frac{L^{d-1}}{z^{d-1}}$, which is infinite at $z = 0$. So, we make the integration at $z = \epsilon$. Also, we say that $\int d^{d-1}x = R^{d-1}$. So, the number of degrees of freedom is $\frac{L^{d-1}}{4G_N}(\frac{R}{\epsilon})^{d-1}$. This number scales the same way with R and ϵ as it did for the quantum field theory.

We now prove that the d dimensional conformal group acting on Minkowski space is isomorphic to the group of symmetry of AdS_{d+1}. This provides another link between conformal field theories in d dimensional Minkowski space and gravity in AdS_{d+1}.

First, we start by defining what is the conformal group. The conformal group is the Lorentz group plus translations, dilatations and special conformal transformations. A special conformal transformation generated by a certain vector b^μ is the transformation $x^\mu \to x'^\mu = \frac{x^\mu - x^2 b^\mu}{1-2b\cdot x+b^2x^2}$. This can be viewed as an

inversion, after a translation, after an inversion, because

$$\frac{x^\mu - x^2 b^\mu}{1 - 2b\cdot x + b^2 x^2} = \frac{\frac{x^\mu}{x^2} - b^\mu}{(\frac{x^\mu}{x^2} - b^\mu)^2}. \tag{48}$$

Let us investigate the size of the d dimensional conformal group. It has $\frac{d(d-1)}{2}$ Lorentz rotations, plus d translations, d special conformal transformations and finally 1 dilatation. So, it has $\frac{(d+1)(d+2)}{2}$ generators, which is the same number that $SO(d,2)$ has.

A representation of the conformal group is

$$\begin{aligned} P_\mu &= -i\partial_\mu, \\ D &= -ix^\mu\partial_\mu, \\ L_{\mu\nu} &= i(x_\mu\partial_\nu - x_\nu\partial_\mu), \\ K_\mu &= -i(2x_\mu x^\nu\partial_\nu - x^2\partial_\mu), \end{aligned} \tag{49}$$

for translations, dilatations, rotations and special conformal transformations, respectively. From this, we can deduce its Lie algebra. The nonzero commutators are

$$\begin{aligned} [D, P_\mu] &= iP_\mu, \\ [D, K_\mu] &= -iK_\mu, \\ [K_\mu, P_\nu] &= 2i(\eta_{\mu\nu}D - L_{\mu\nu}), \\ [K_\rho, L_{\mu\nu}] &= i(\eta_{\rho\mu}K_\nu - \eta_{\rho\nu}K_\mu), \\ [P_\rho, L_{\mu\nu}] &= i(\eta_{\rho\mu}P_\nu - \eta_{\rho\nu}P_\mu), \\ [L_{\mu\nu}, L_{\rho\sigma}] &= i(\eta_{\nu\rho}L_{\mu\sigma} + \eta_{\mu\sigma}L_{\nu\rho} - \eta_{\mu\rho}L_{\nu\sigma} - \eta_{\nu\sigma}L_{\mu\rho}). \end{aligned} \tag{50}$$

The generators of $SO(d,2)$ form an antisymmetric tensor J_{AB}, with Lie algebra

$$[J_{AB}, J_{CD}] = i(\eta_{AD}J_{BC} + \eta_{BC}J_{AD} - \eta_{AC}J_{BD} - \eta_{BD}J_{AC}), \tag{51}$$

where uppercase latin indices go from 1 to $d+2$ and the metric η_{AB} is diagonal with signature $\{-1,+1,...,+1,-1\}$.

Finally, we show how to construct from (50) an antisymmetric tensor J_{AB}

such that (51) is obeyed. Define

$$\begin{aligned} J_{\mu\nu} &= L_{\mu\nu}, \\ J_{d+1,\mu} &= \frac{K_\mu + P_\mu}{2}, \\ J_{d+2,\nu} &= \frac{K_\mu - P_\mu}{2}, \\ J_{d+1,d+2} &= D, \end{aligned} \tag{52}$$

where the greek indices go from 1 to d and we define J_{AB} to be antisymmetric. It is now a straightforward algebraic computation to show that (51) is satisfied. This proves that indeed the d dimensional conformal group acting on Minkowski space is isomorphic to $SO(d,2)$.

Suppose we want to calculate the correlation function

$$< T\{O_1(x_1)...O_n(x_n)\} > \tag{53}$$

of a certain quantum field theory on a fixed background metric. One way of doing that is to add to the lagrangian $L(x)$ the functions $\sum_{i=1}^{n} J(x)O_i(x)$ and then use

$$< T\{O_1(x_1)...O_n(x_n)\} >= \frac{1}{Z_0}(-i\frac{\delta}{\delta J(x_1)})...(-i\frac{\delta}{\delta J(x_n)})Z[J]_{J=0}, \tag{54}$$

where $Z[J]$ is the generating functional obtained by the substitution $L(x) \rightarrow L(x) + \sum_{i=1}^{n} J(x)O_i(x)$.

If the background metric is not fixed, like in a quantum theory of gravity, then in the path integral we must also sum over different metrics. The statement of AdS/CFT is that, under some assumptions, the generating functional of a conformal field theory in d dimensional Minkowski space is equal to the generating functional of a gravity theory in an asymptotically AdS_{d+1} space.

Furthermore, this duality is often of the strong/weak coupling type and of the quantum/classical type. By that, we mean that it often relates quantum field theories with strong coupling to classical theories of gravity with weak coupling. This means that we can, to good approximation, compute the generating functional on the gravity side by just picking the most probable path and computing $\exp(iS_{grav}(g_{\mu\nu}, \phi_1, \phi_2, ...))$, where $g_{\mu\nu}, \phi_1, \phi_2, ...$ are the field configurations which solve the equations of motion. Using that, we can then calculate functional derivatives and compute correlation functions. The calculation of

$S_{grav}(g_{\mu\nu}, \phi_1, \phi_2, ...)$ usually involves careful regularization of infinities related to integrations on the conformal boundary[8].

We now derive an important result to our later investigations. In this thesis, we are studying an asymptotically AdS spacetime. So, near the conformal boundary where $z = 0$, the metric is always

$$ds^2 = \frac{L^2}{z^2}(\eta^{\mu\nu}dx_\mu dx_\nu + dz^2), \tag{55}$$

where $\eta^{\mu\nu}$ is the minkowski metric in d dimensions and we are studying AdS space in $d+1$ dimensions. Let us write the KG equation $\Box\psi - m^2\psi = 0$ using this metric

$$\frac{z^2}{L^2}(\partial_z^2\psi + \eta^{\mu\nu}\partial_\mu\partial_\nu\psi) - (d-1)\frac{z}{L^2}\partial_z\psi - m^2\psi = 0. \tag{56}$$

We decompose the scalar field in fourier components

$$\psi(z, x) = \exp(ik \cdot x) f_k(z) \tag{57}$$

and the KG equation becomes

$$z^2 f_k''(z) - (d-1)z f_k'(z) - (k^2 z^2 + m^2 L^2) f_k(z) = 0. \tag{58}$$

Near $z \sim 0$, $k^2z^2 + m^2L^2 \sim m^2L^2$. Equation (58) suggests a power law solution. We try $f_k(z) = z^\Delta$ and we get that the equation is satisfied provided $\Delta = \frac{d}{2} \pm \sqrt{(\frac{d}{2})^2 + m^2L^2}$.

For our present case, plugging $d = 3$ (spacetime is in dimensions $d+1$) and $m^2 = -\frac{2}{L^2}$ in the last formula[9], we obtain $\Delta_- = 1$ and $\Delta_+ = 2$. So, near $z \sim 0$

$$\phi(z, x) = \phi_1(x)z + \phi_2(x)z^2. \tag{59}$$

The gauge-gravity duality provides a physical meaning to the quantities $\phi_1(x)$ and $\phi_2(x)$. Introducing a scalar field in the gravity theory, corresponds in the CFT to adding a source term $\int d^dx J(x)O(x)$ to the action, where $J(x)$ is

[8] See [8] for details on this point.

[9] Despite being negative, the mass is above the BF bound, so it induces no instability.

a function we choose (that's why we call it a source) and $O(x)$ is a scalar operator. The gauge gravity duality says that $\phi_1(x) = J(x)$ and $\phi_2(x) = \langle O(x) \rangle$, where $\langle O(x) \rangle$ is the expectation value for the operator $O(x)$[10].

5 Hovering Black Holes from Charged Defects

Given the great influence it has on our work, we summarize here the main points of [1]. In this paper, solutions of the Einstein-Maxwell equations with a negative cosmological constant were studied, imposing the following boundary conditions. First, it was demanded that spacetime becomes AdS near the conformal boundary. The second condition is that near $z \sim 0$ the maxwell field A_μ becomes equal to just $\mu(r)dt$, where $\mu(r)$ is a function we choose. In [1], only localized defects were studied, that is, $\mu(r) \to 0$ as $r \to \infty$.

[1] considered profiles where $\mu(r)$ goes like $\frac{a}{r^\beta}$, at infinity. Using units where $c = \hbar = 1$, this means that a has dimensions $[E]^{1-\beta}$. So, if $\beta < 1$, we will say that $\mu(r)$ is a relevant profile, if $\beta = 1$, it is a marginal profile and if $\beta > 1$, it is irrelevant. The reason for this definition is the following. When the profile is irrelevant, the IR horizon is the usual Poincaré horizon, i.e. it is exactly equal to AdS spacetime there. The IR horizon is the region farther away from the conformal boundary, so in this case this means that the irrelevant profile isn't *strong* enough to deform spacetime there. By contrast, for the marginal profile the IR horizon is deformed. Relevant profiles would deform spacetime in the IR horizon so much, that they weren't studied (their metric there would be very different from AdS)[11].

The authors considered the cases where $\mu(r)$ is marginal and irrelevant. It turns out that for a large class of profiles in both cases, for sufficiently large a, a Reissner-Nördstrom AdS black hole is formed in the bulk. For increasing a, the size of the black hole grows. They could find in this way very large black

[10] A generalization of this is possible for n-point correlation functions.

[11] Let us clarify the meaning of this classification with regards to our own work. We study a massive scalar field, which is a relevant operator in the dimension we're in. Near the conformal boundary, this scalar field goes like $z\phi_1(r)$, where $\phi_1(r)$ is just some function, which we call a profile. According to its decay with $r \to \infty$, we say that this profile may be relevant, marginal or irrelevant. This does not change the fact that the scalar field is a relevant operator.

hole solutions, as large as $3L$, where L is the AdS radius.

Let $a*$ be the value of a for which a black hole is formed for a certain profile. The main finding of the paper is that, for every profile that exhibits a black hole, the black hole size increases always the same way with $a/a*$. The details of the profile are irrelevant. An explanation for this universality was not provided.

The point of our work was, instead of introducing a boundary maxwell field, studying instead a scalar field.

6 Setup

We study gravity with a scalar field described by the action

$$S = \frac{1}{G}\int d^4x\sqrt{-g}(R - 2\Lambda + 4V(\Phi) + 2\nabla\Phi\cdot\nabla\Phi), \tag{60}$$

where $V(\Phi) = \frac{1}{2}m^2\Phi^2$ and $\Lambda = -\frac{(d-1)(d-2)}{2L^2} = -\frac{3}{L^2}$. Note that Φ is dimensionless. This gives rise to the following equations of motion

$$G_{\mu\nu} + \frac{3}{L^2}g_{\mu\nu} - \Big(2\partial_\mu\Phi\partial_\nu\Phi + 2V(\Phi)\Big) = 0. \tag{61}$$

We choose $m^2 = -\frac{2}{L^2}$. Despite being negative, the mass is above the BF bound, so it induces no instability. This particular value is chosen so that it coincides with the mass of a scalar field conformally coupled to the curvature of AdS_4 space. Such a field has a mass[12]

$$m^2 = \xi(d)R = \frac{d-2}{4(d-1)}\frac{d(1-d)}{L^2} = -\frac{d(d-2)}{4L^2} = -\frac{2}{L^2}. \tag{62}$$

We can now write the ansatz to solve these equations. In order to understand where it comes from, we start by rewriting the metric of the Poincaré patch of AdS space as

$$ds^2_{AdS_4} = \frac{L^2}{z^2}(-dt^2 + dz^2 + dr^2 + r^2d\phi^2). \tag{63}$$

Let us define the polar coordinates $z = \rho\cos\theta, r = \rho\sin\theta$. Then,

$$ds^2_{AdS_4} = \frac{L^2}{\cos^2\theta}(\frac{-dt^2 + d\rho^2}{\rho^2} + d\theta^2 + \sin^2\theta d\phi^2). \tag{64}$$

[12] I do not know a reference for this, but it was proven in the course *Topics in Theoretical Physics* in the classes taught by João Penedones.

Defining $\rho = \frac{1}{\eta}$

$$ds^2_{AdS_4} = \frac{L^2}{\cos^2\theta}(-\eta^2 dt^2 + \frac{d\eta^2}{\eta^2} + d\theta^2 + \sin^2\theta d\phi^2). \tag{65}$$

This way, AdS_4 is foliated by $\eta = const$ slices which are conformal to $\Re \times S^2$. Notice that there is now a zero temperature horizon at $\eta = 0 \leftrightarrow z = \infty, r = \infty$. We call this an IR horizon.

When doing numerical work involving spectral methods, it is convenient to deal with polynomials instead of trigonometric functions. We define an angular coordinate x by $\cos\theta = 1 - x^2, x \in [0,1]$. Besides, we define a new variable y by $\rho = L\frac{1-y^2}{y\sqrt{2-y^2}}, y \in [0,1]$.

$$ds^2_{AdS_4} = \frac{L^2}{(1-x^2)^2}\big(-\frac{y^2(2-y^2)}{(1-y^2)^2}dt^2 + \frac{4}{y^2(1-y^2)^2(2-y^2)^2}dy^2 + \frac{4}{2-x^2}dx^2 + x^2(2-x^2)d\phi^2\big) \tag{66}$$

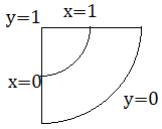

Figure 5: Poincaré Patch in the new coordinates. The IR horizon is at $y = 0$. $y = 1$ is just a point (the corner). The conformal boundary is at $x = 1$ or $y = 1$. The axis is at $x = 0$.

The conformal boundary is at $x = 1$ or $y = 1$. Since the metric of our system (with the scalar field) must be asymptotically AdS_4, stationary and axisymmetric, we choose the following ansatz

$$ds^2 = \frac{L^2}{(1-x^2)^2}\big(-\frac{y^2(2-y^2)}{(1-y^2)^2}q_1(y,x)dt^2 + \frac{4}{y^2(1-y^2)^2(2-y^2)^2}q_2(y,x)dy^2 + \frac{4}{2-x^2}q_3(y,x)(dx - x\frac{q_5(y,x)}{y}dy)^2 + x^2(2-x^2)q_4(y,x)d\phi^2\big). \tag{67}$$

The function $q_5(y,x)$ allows for a crossed term in the metric. Near the conformal boundary, the scalar field Φ must go like $\Phi(z,r) \sim z\phi(r)$, where $\phi(r)$ is a certain profile we choose. We study profiles that decay like $\frac{\phi_B}{r^\beta}$. ϕ_B has dimensions of $[E]^{1-\beta}$ and so it is said to be relevant if $\beta < 1$, marginal if $\beta = 1$ and irrelevant if $\beta > 1$. Since $z = \rho(1-x^2)$, we choose the following ansatz for the scalar field

$$\Phi = (1-x^2)q_6(y,x) \tag{68}$$

This makes our life easier when imposing boundary conditions for the scalar field at the conformal boundary. We remark that the total number of PDE's that this procedure originates is 6.

7 Boundary Conditions

7.1 Conformal Boundary

The conformal boundary is at $x=1$ or $y=1$. So, at those places, we put $q_1 = q_2 = q_3 = q_4 = 1$, $q_5 = 0$. The condition for q_6 is $q_6 = L\frac{1-y^2}{y\sqrt{2-y^2}}\phi(L\frac{1-y^2}{y\sqrt{2-y^2}})$, where ϕ is the profile that we are considering. At $y=1$, $q_6 = \lim_{\epsilon\to 0}\epsilon\phi(\epsilon)$[13]. An important distinction between the marginal and irrelevant case occurs when we consider the boundary condition for q_6 at $x=1, y=0$. This corresponds to $r\to\infty$. For the marginal case, $q_6 = \phi_0$, for the irrelevant case, $q_6 = 0$. We will see that this is important for the IR horizon.

7.2 Regularity Condition at $x=0$

We need to impose boundary conditions at $x=0$ and $y=0$. These come from the fact that we assume all the fields q_i to be analytic functions. We Taylor expand the equations of motion around $x=0$ and impose that the zeroth and first order terms be null. We obtain from this that $q_1^{(0,1)}(y,0)$, ${q_2}^{(0,1)}(y,0)$, $q_4(y,0)-q_3(y,0), q_4^{(0,1)}(y,0), q_5^{(0,1)}(y,0)$ and $q_6^{(0,1)}(y,0)$ are null.

7.3 IR Horizon: irrelevant profile

We consider now the boundary conditions for $y=0$. Unlike the $x=0$ case, we obtain a set of second order non linear ODE's in the variables $q_1(0,x),...,q_6(0,x)$. The boundary conditions are the ones we already obtained when we considered the $x=0$ and $x=1$ case, i.e., at $x=0$ all the x derivatives are null and

[13] If $\phi(r) = \frac{\phi_0}{r}$, then the boundary condition is $q_6 = \phi_0$.

$q_3 = q_4$ and at $x = 1$, $q_1 = q_2 = q_3 = q_4 = 1$, $q_5 = 0$ [14]. In the irrelevant profile, $q_6 = 0$ at $x = 1$. Notice that there can be only one solution that solves the set of ODE's and respects the boundary conditions.

The simplest guess is to try $q_1(0, x) = q_2(0, x) = q_3(0, x) = q_4(0, x) = 1$, $q_5(0, x) = q_6(0, x) = 0$. It clearly obeys the boundary conditions. It turns out that it also solves the set of ODE's, so it is the solution we are looking for. This has a simple interpretation: when the profile is irrelevant it decays quickly and so it does not change the IR horizon, which is still the usual Poincaré horizon. We bring attention to the fact that the conformal boundary is connected to the IR horizon at $x = 1, y = 0 \Leftrightarrow z = 0, r \to \infty$, i.e., exactly at the place where the decay of the profile should be most relevant.

7.4 IR Horizon: marginal profile

In the marginal case, $q_6 = \phi_0$ at $x = 1$, so the solution for the irrelevant profile is no longer valid[15]. We solved the set of ODE's numerically, according to the methods explained in section 3.

After knowing $q_1(0, x)$, ... $q_6(0, x)$, we did a Taylor expansion of scalars like the curvature, the kretchmann and the norm of the Weyl tensor around $y = 0$ and calculated the zeroth order term. We graph the maximum along x of all these three quantities as a function of ϕ_B, as you can see in figures (6), (7) and (8).

Scalars like the Kretchmann and the curvature increase with ϕ_B, which makes sense since the energy momentum tensor goes with ϕ_B^2. More surprisingly, $W^2 \equiv W_{abcd}W^{abcd}$, where W_{abcd} is the Weyl tensor, tends to a constant for large Φ. As we show in Appendix C, this means that the degrees of freedom contained in the Riemann tensor, which do not depend on the matter field energy momentum tensor, are becoming fixated. We can interpret this as having the metric changing as little as possible with ϕ_B, given the constraint that the Einstein equations must be obeyed.

[14] This can also be seen by taking the non linear ODE's and Taylor expanding around $x = 0$ and $x = 1$.

[15] This set of ODE's has another interesting property. Suppose we take the original Einstein equations and now assume that the fields q_i, $i = 1, ..., 6$ only depend on x. The equations we obtain turn out to be exactly the same as the set of ODE's we are considering here.

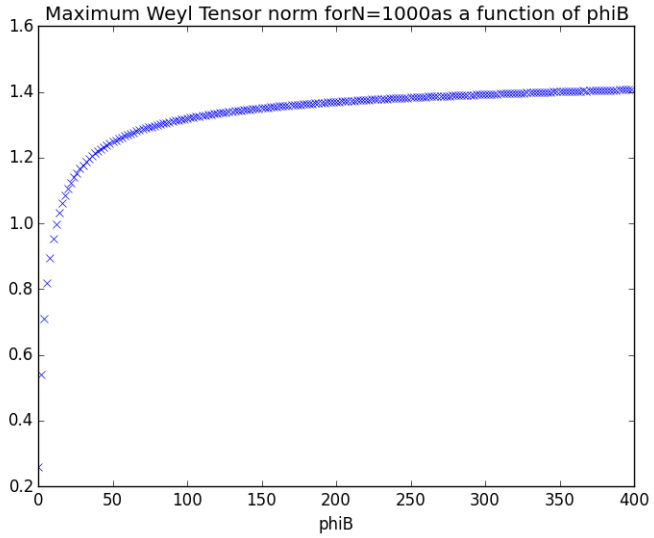

Figure 6: Maximum of the Contraction of the Weyl Tensor in the IR horizon as a function of ϕ_B

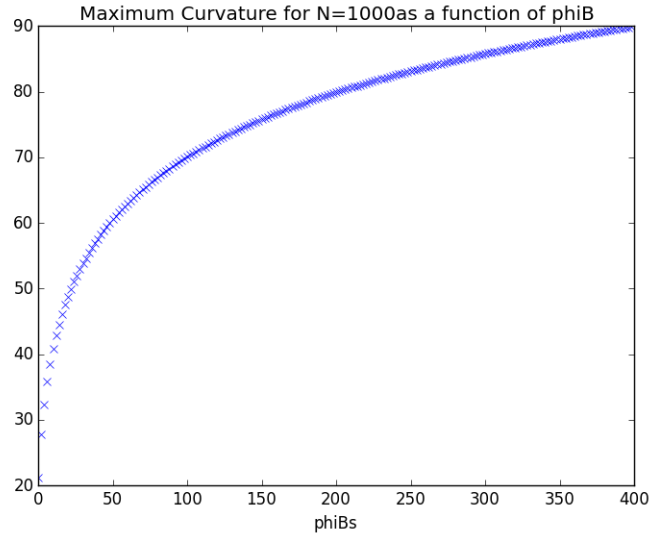

Figure 7: Maximum of the Curvature in the IR horizon as a function of ϕ_B

As a check on our numerical analysis, we performed a perturbative calculation for small ϕ_B. See figure 9 for the result and appendix **A** for the details regarding this computation.

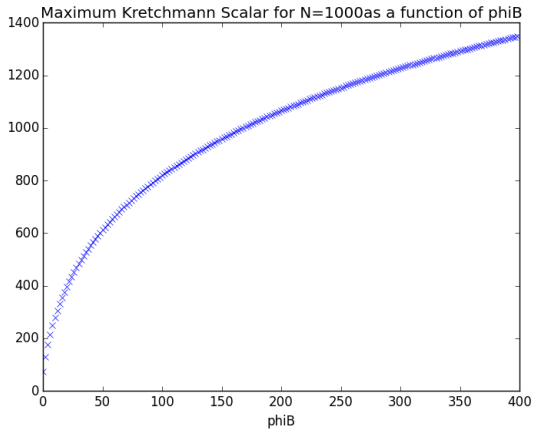

Figure 8: Maximum of the Kretchmann Scalar in the IR horizon as a function of ϕ_B

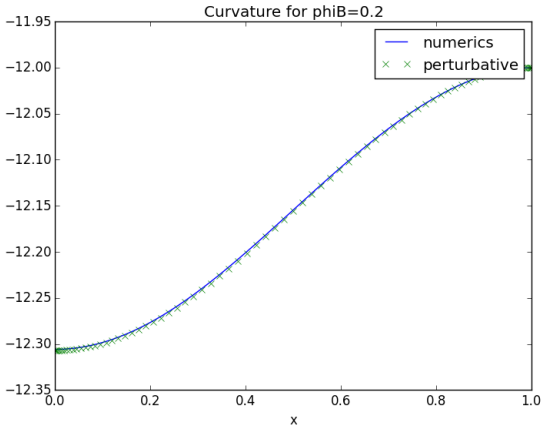

Figure 9: Curvature in the IR horizon for $\phi_B = 0.2$. The agreement between numerical and perturbative methods is total.

8 Bulk Spacetime

[16]Having discussed the issue of what boundary conditions to impose, we turn our attention to the numerical solution of the Einstein equations in the bulk. For concreteness, we focus on the irrelevant profile $\phi(r) = \frac{\phi_B}{(\sigma^2+r^2)^{\frac{3}{2}}}$, with $\sigma = 1$ in units of L. Like in section 7.4, we can see in figures 10 and 11 how the

[16]Marvin Silva provided some useful computer support here.

maximum value of scalars like the curvature or the Kretchmann scalar increase with ϕ_B. In figure 12, we sketch the evolution with ϕ_B of the norm of the deTurck vector.

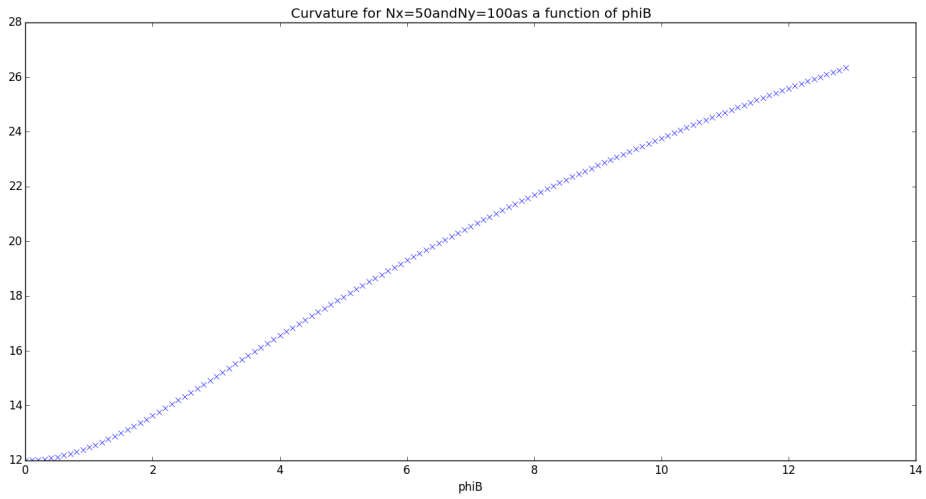

Figure 10: Maximum of the Curvature in the bulk as a function of ϕ_B. As expected, it increases with ϕ_B.

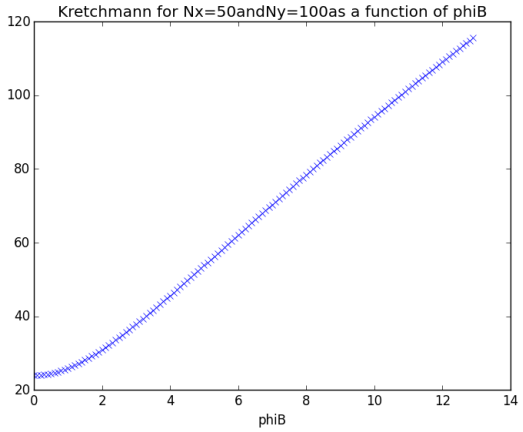

Figure 11: Maximum of the Kretchmann scalar in the bulk as a function of ϕ_B. As expected, it increases with ϕ_B.

A major difficulty in our numerical work is that the norm of the deTurck vector increases with ϕ_B. A way to counter this is to use larger grids for increasing

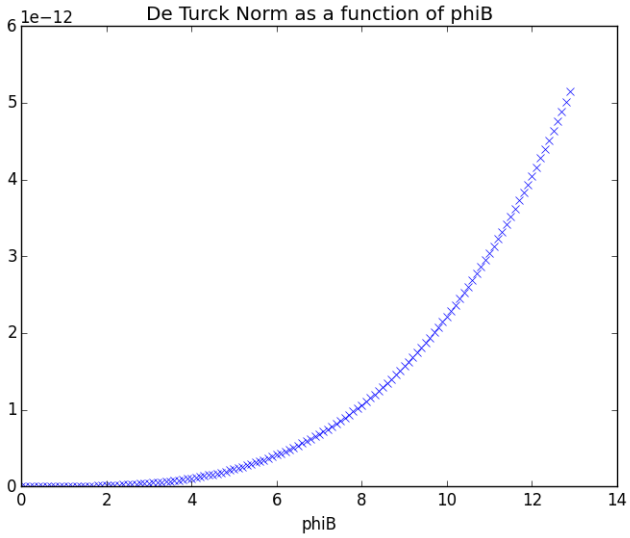

Figure 12: Maximum of the norm of the deTurck vector in the bulk as a function of ϕ_B. It is always below the threshold we imposed of $10^{-10}L^{-2}$.

ϕ_B. Because of the computational cost, we were unable to get reliable results beyond $\phi_B \sim 14$.

The maximum of the contraction of the Weyl tensor in the bulk also increases with ϕ_B for the range of values we're considering. See figure 13.

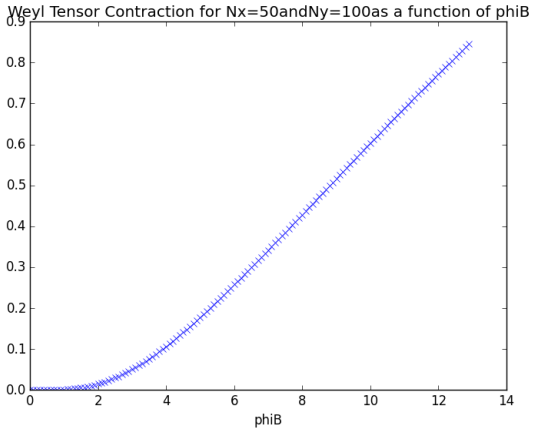

Figure 13: Maximum of the contraction of the Weyl Tensor in the bulk as a function of ϕ_B.

It is also interesting to investigate the spatial distribution of scalars along the Poincaré patch. See figure 14, for the case of the curvature.

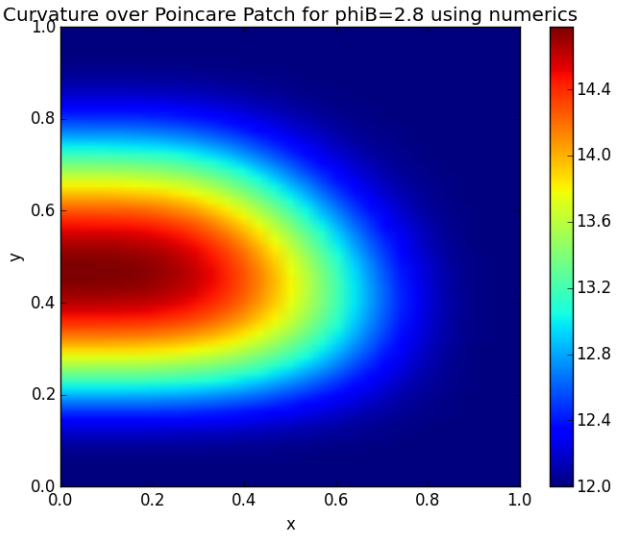

Figure 14: Absolute value of the curvature. It attains its maximum for $x = 0$ and y in between 0 and 1.

In analogy to [1], we investigate whether a small AdS-Schwarzschild black hole is formed. It should behave like a particle on a background metric. We thus ask if the metric allows at any ϕ_B a static geodesic, that is, a particle that only moves in the t direction, in our present coordinate system. More precisely, if the particle's velocity is $(\frac{1}{\sqrt{-g_{tt}}}, 0, 0, 0)$, is it ever possible that $u^\nu \nabla_\nu u^\mu = 0$? Symmetry suggests that, if this is to happen, it should happen at the axis at $x = 0$, because at $x \neq 0$ the particle needs to choose a certain φ to be in and there's symmetry in φ[17]. Also, we calculated scalars like the curvature and the Kretchmann and they all attain their maximum at $x = 0$. Because of this, we focus on $x = 0$.

Remembering now that $\frac{\partial}{\partial t}$ is a Killing vector and the regularity conditions at $x = 0$, $\partial_x g_{tt} = 0$ and $g^{xy} = 0$, the only nonzero component of $u^\nu \nabla_\nu u^\mu$ is the y component, which gives

[17] By φ here we mean the angular coordinate and not the scalar field. Hopefully one can tell from context.

$$\frac{1}{2}\frac{1}{(-g_{tt})}g^{yy}\partial_y(-g_{tt}) \tag{69}$$

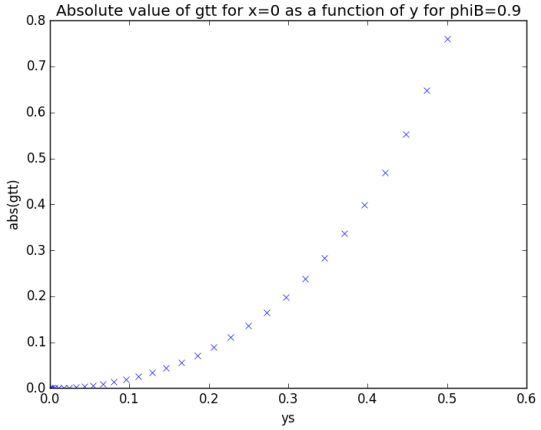

Figure 15: g_{tt} has no maximum, nor minimum, i.e. $\partial_y g_{tt}$ is never null at $x = 0$. This remains the case for all values of ϕ_B that we have studied.

So, we expect that there is no AdS-Schwarzschild black hole.

We check our numerical work with a perturbative calculation (see appendix **B** for details).

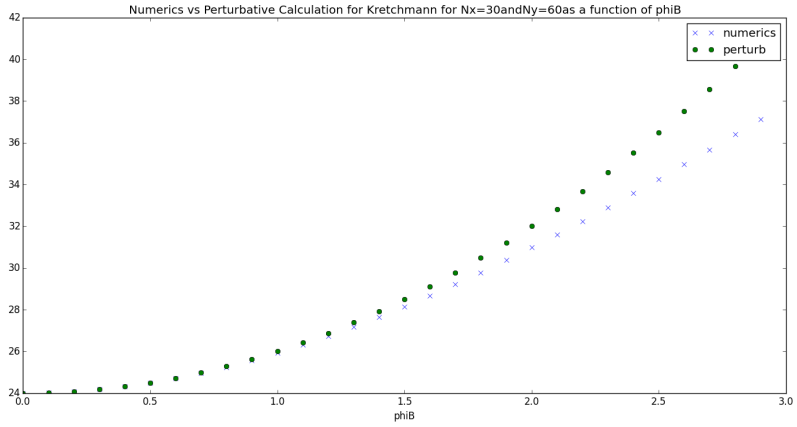

Figure 16: Maximum of the Kretchmann Scalar in the bulk spacetime computed using numerics and perturbative methods. For small ϕ_B there's perfect agreement.

9 Discussion and Further Work

Our present work is still very incomplete and there are still a lot of relevant questions to ask. Is there a value of ϕ_B above which we can not find a solution to the Einstein equations, just like in [1]? In the limit $\phi_B \to \infty$, does the maximum of the contraction of the Weyl Tensor in the bulk tend to a constant, just like it happens in the IR horizon? We need to extend the calculation we have done in section 8 for larger values of ϕ_B in order to answer these questions. Besides, we should consider other profiles and see if the conclusions from section 8 still hold, namely if an AdS-Schwarzschild black hole is still absent[18].

It would be interesting to consider a similar scenario to this one, where instead of adding a scalar field to AdS space, we add a scalar field to planar AdS Schwarzschild spacetime. One difference now is that the IR horizon possesses a certain temperature[19].

We have seen that the maximum of the contraction of the Weyl Tensor tends to a constant with larger ϕ_B in the IR horizon and we hypothesize that this is true in the bulk as well. That would mean that the Riemann tensor is getting as constant as it can, while still satisfying the Einstein equations for different values of ϕ_B. We could certainly gain a lot of knowledge if we could obtain an analytical expression for the metric in the limit $\phi_B \to \infty$.

More broadly speaking, there are further problems we could takle which are related to this study. One of them is generalizing the deTurck gauge for non stationary spacetimes. This would be very helpful, as it would enable us to study gravity in AdS space in a dynamical setting using spectral methods.

Appendix

A - Perturbative Calculation for ODE's

We calculate the metric for small ϕ_B. Our method is the following. First, we use the metric of AdS space and write with it the Klein Gordon equation for

[18] We have already made some numerical calculations and until now that conclusion still holds, but a systematic study is needed.

[19] The study of a maxwell field coupled to a charged complex scalar field in planar AdS Schwarzschild has already been fruitfully carried out in [9] and [10].

the scalar field. We solve this equation to linear order in ϕ_B. Armed with this knowledge, we calculate the energy momentum tensor to order ϕ_B^2. Now we solve the Einstein equations to order ϕ_B^2, i.e., we obtain the metric to order ϕ_B^2. We have now gone full circle and we can use the metric to order ϕ_B^2 to obtain the scalar field to order ϕ_B^3 and then use that to obtain the metric to order ϕ_B^4 and so on... The point here is that the energy momentum tensor $T_{\mu\nu}$ is quadratic in the scalar field Φ,

$$T_{\mu\nu} = -g_{\mu\nu}\big(\partial\Phi\cdot\partial\Phi + 2V(\Phi)\big) + 2\partial_\mu\Phi\partial_\nu\Phi. \tag{70}$$

We will now explain this procedure more carefully. First, we remark that not all the six fields $q_i, i = 1, ..., 6$ are non zero and independent at the IR horizon. In fact, $q_5(0, x) = 0$ and $q_1(0, x) = q_2(0, x)$[20]. Redefining $q_3 \to q_2$ and $q_4 \to q_3$, let us write[21]

$$q_1(x) = 1 + a_1(x)\phi_B + a_2(x)\phi_B^2 + ... \tag{71}$$

$$q_2(x) = 1 + b_1(x)\phi_B + b_2(x)\phi_B^2 + ... \tag{72}$$

$$q_3(x) = 1 + c_1(x)\phi_B + c_2(x)\phi_B^2 + ... \tag{73}$$

$$\Phi(x) = d1(x)\phi_B + d2(x)\phi_B^2 + ... \tag{74}$$

Since at $x = 1$ spacetime must be AdS, $a_i(1) = b_i(1) = c_i(1) = 0$. Also, at $x = 0$ we impose the regularity conditions written in section 7.2.

Using this, we can now make similar expansions for the energy momentum tensor, the metric, the box operator and the Riemann tensor, with the result

$$T_{\mu\nu} = T^{(2)}_{\mu\nu}\phi_B^2 + T^{(3)}_{\mu\nu}\phi_B^3 + T^{(4)}_{\mu\nu}\phi_B^4 + ... \tag{75}$$

$$g_{\mu\nu} = g^{(0)}_{\mu\nu} + g^{(1)}_{\mu\nu}\phi_B + g^{(2)}_{\mu\nu}\phi_B^2 + g^{3}_{\mu\nu}\phi_B^3 + ... \tag{76}$$

$$\Box = \Box^{(0)} + \Box^{(1)}\phi_B + \Box^{(2)}\phi_B^2 + ... \tag{77}$$

$$R_{\mu\nu} = R^{(0)}_{\mu\nu} + R^{(1)}_{\mu\nu}\phi_B + R^{(2)}_{\mu\nu}\phi_B^2 + R^{(3)}_{\mu\nu}\phi_B^3 + R^{(4)}_{\mu\nu}\phi_B^4 + ... \tag{78}$$

Let us see how this works explicitly to order 2. At the beginning, we only know

[20] I know that I can solve the set of ODE's by imposing these conditions, but I'm unaware of a physical reason why this must be true.

[21] In this case, it is not convenient to put $\Phi = (1 - x^2)q_6(x)$

all the zeroth order terms. The KG equation to linear order is

$$(\Box^{(0)} - m^2)\Phi^{(1)}(x) = 0, \tag{79}$$

with the boundary conditions that $\Phi^{(1)}(x)$ goes like $1 - x^2$ near $x = 1$[22] and the derivative of $\Phi^{(1)}(x)$ at $x = 0$ equals 0. We solve this ODE and obtain $\Phi^{(1)}(x) = 1 - x^2$.

The Einstein equations, to linear order, are

$$G^{(1)}_{\mu\nu} + \Lambda g^{(1)}_{\mu\nu} = 0. \tag{80}$$

The boundary conditions are that $g^{(1)}_{\mu\nu}$ must be null at the conformal boundary and that it should obey the regularity conditions at $x = 0$. The equations (80) are a homogeneous set of ODE's, i.e., they contain no source term. Together with the boundary conditions, they imply $g^{(1)}_{\mu\nu} = 0$. Hence, $\Box^{(1)} = 0$.

The KG equation to second order is

$$(\Box^{(0)} - m^2)\Phi^{(2)} = -\Box^{(1)}\Phi(1), \tag{81}$$

with the boundary conditions that $\Phi^{(2)}$ is null at $x = 1$ and its derivative is zero at $x = 0$. Also, the rhs of (81) is null, since $\Box^{(1)} = 0$. So, $\Phi^{(2)} = 0$.

We can now obtain $T^{(2)}_{\mu\nu}$. Writing the Einstein equations to second order, we will obtain a non homogeneous set of ODE's for $g^{(2)}_{\mu\nu}$. The equations are

$$\begin{aligned}
&8x(x^2-1)^2 a_2(x) - 8x(x^4 - 2x^2 - 2)b_2(x) + (x^2-1)\Big((-5x^4 + 11x^2 + 2)a_2'(x) \\
&+x\big((x^2-1)((x^2-2)a_2''(x) + 16) + 2x(x^2-2)b_2'(x) - 2x(x^2-2)c_2'(x)\big)\Big) = 0 \\
&24xb_2(x) + (x^2-1)\left(4a_2'(x) - 2b_2'(x) + 4c_2'(x) + 16x^3 - 16x\right. \\
&\left. x^5 c_2''(x) - 3x^3 c_2''(x) + 2xc_2''(x) - x^4 c_2'(x) + 3x^2 c_2'(x)\right) = 0 \\
&-2x\left(x^2-1\right)^2 a_2(x) + 2x\left(x^4 - 2x^2 - 2\right)b_2(x) + \left(x^2-1\right) \\
&\left(x^4 - 2x^2 - 1\right)a_2'(x) + x\left(x\left(x^2-2\right)c_2'(x) + 2\left(x^6 - 3x^4 + 2\right)\right) = 0
\end{aligned} \tag{82}$$

These equations are not elliptic, as a $b''(x)$ term is missing. Notice we have not imposed the deTurck gauge, so this is natural. Let's solve the third equation for $b_2(x)$ and plug that into the first two equations.

[22] This amounts to demanding that near the conformal boundary, the scalar field goes like $z\phi_1(r)$ where $\phi_1(r)$ is the profile we are considering. See section 4.

$$
\begin{aligned}
b_2(x) = -\frac{1}{2x\left(x^4-2x^2-2\right)}(x^2-1)\left(-2x\left(x^2-1\right)a_2(x)\right.\\
\left.+\left(x^4-2x^2-1\right)a_2'(x)+x\left(x\left(x^2-2\right)c_2'(x)+2\left(x^6-3x^4+2\right)\right)\right)\\
\left(-1+x^2\right)\left(24x^3\left(x^2-1\right)a_2(x)\right.\\
\left.+\left(-9x^6+19x^4+4x^2-2\right)a_2'(x)+x\left(-x\left(x^8-5x^6+10x^4-6x^2+12\right)c_2'(x)\right.\right.\\
\left.\left.+\left(x^6-3x^4+2\right)\left(a_2''(x)+\left(x^2-2\right)x^2c_2''(x)\right)\right)\right)=0\\
\left(1+x^2-3x^4+x^6\right)\left(24x^3\left(x^2-1\right)a_2(x)\right.\\
\left.+\left(-9x^6+19x^4+4x^2-2\right)a_2'(x)+x\left(-x\left(x^8-5x^6+10x^4-6x^2+12\right)c_2'(x)\right.\right.\\
\left.\left.+\left(x^6-3x^4+2\right)\left(a_2''(x)+\left(x^2-2\right)x^2c_2''(x)\right)\right)\right)=0.
\end{aligned}
\tag{83}
$$

Clearly, the last two equations are equivalent. To make progress, we must choose a gauge. Our philosophy during this section will be to impose a gauge order by order. That way, we can look at the equations and choose. We put $c_2(x) = -\alpha a_2(x)$. To order 2, α is a gauge variable, i.e., when we calculate scalars like the curvature or the kretchmann they will not depend on α to order 2. Yet, if we want to proceed with the calculation to higher order, we will have to fix α, so in that sense it is not a gauge variable. Solving the equations (83) and imposing the boundary conditions, we obtain

$$
\begin{aligned}
a2(x) = -\frac{(x^2-1)^3}{2\alpha x^4-4\alpha x^2-2},\\
b2(x) = -\frac{1}{\left(-\alpha x^4+2\alpha x^2+1\right)^2}\left(x^2-1\right)^2\left(\frac{1}{2}(-\alpha-2)+1\right.\\
\left.\alpha^2x^8-\frac{7\alpha^2x^6}{2}+\left(\frac{5\alpha}{2}-2\right)\alpha x^4-\left(-\alpha^2-\frac{9\alpha}{2}-1\right)x^2\right),\\
c2(x) = \frac{\alpha\left(x^2-1\right)^3}{2\alpha x^4-4\alpha x^2-2}.
\end{aligned}
\tag{84}
$$

No new methods are involved in going to higher orders, so we will not show the details here. We calculated expressions up to order 4. In order 5, we started to encounter dilogarythms and so we stopped.

As we have seen, for $\phi_B = 0.2$ this expansion works well. For larger values, it starts to work worse, as we illustrate in figure 17.

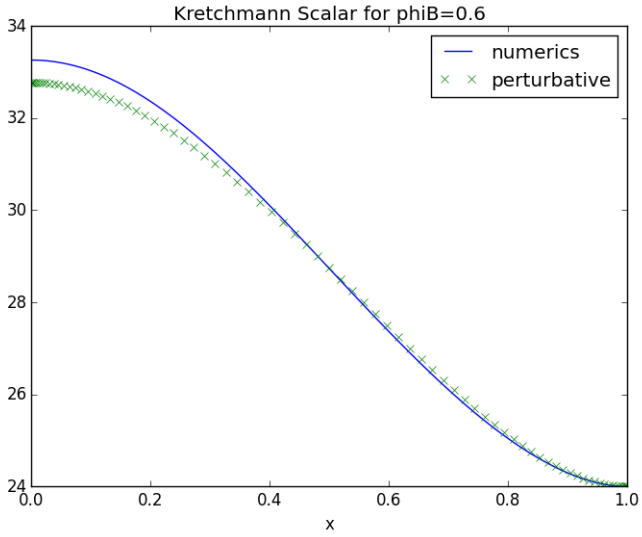

Figure 17: Kretchmann Scalar in the IR horizon for $\phi_B = 0.6$. Near the conformal boundary ($x = 1$) there's agreement between numerics and the perturbative calculation, for we demand spacetime to be AdS over there.

B - Perturbative Calculation for PDE's

Our method is the same as in Appendix **A**, but now we deal with PDE's and not ODE's. Our calculation is entirely similar to the one in [1] and we emulate most of the steps there.

We start with the ansatz

$$ds^2 = \frac{L^2}{z^2}(-G(r,z)dt^2 + B(r,z)dr^2 + CC(r,z)r^2 d\phi^2 + dz^2). \tag{85}$$

We want to go up to second order, so we write

$$B(r,z) = 1 + b(r,z)\phi_B^2, \tag{86}$$

$$G(r,z) = 1 + g(r,z)\phi_B^2, \tag{87}$$

$$CC(r,z) = 1 + c(r,z)\phi_B^2, \tag{88}$$

$$\Phi(r,z) = \phi_B \phi(r,z) \tag{89}$$

and now we must find b, g, c and $\phi(r,z)$. The KG equation is

$$z\left(z\left(r\phi^{(0,2)}(r,z)+\phi^{(1,0)}(r,z)+r\phi^{(2,0)}(r,z)\right)-2r\phi^{(0,1)}(r,z)\right)+2r\phi(r,z)=0. \tag{90}$$

We need to pick a profile to study. We will study the following irrelevant profile $\frac{\sigma}{(r^2+\sigma^2)^{3/2}}$. The solution to the KG equation that respects this profile is $\frac{z(\sigma+z)}{(r^2+(\sigma+z)^2)^{3/2}}$. We can obtain it by separating variables, demanding that the solution decays as $z\to\infty$ and solving a Bessel differential equation.

We now turn our attention to the Einstein equations to second order in ϕ_B. The zz equation is

$$\begin{aligned}&z(b^{(0,1)}(r,z)-zb^{(0,2)}(r,z)+c^{(0,1)}(r,z)\\&-zc^{(0,2)}(r,z)+g^{(0,1)}(r,z)-zg^{(0,2)}(r,z)-4z\phi^{(0,1)}(r,z)^2)+4\phi(r,z)^2=0,\end{aligned} \tag{91}$$

where $\phi(r,z)$ is the linear order scalar field (that we already know). Notice that defining a variable $c(r,z)+g(r,z)+b(r,z)$, this is an ODE in that variable. We solve this equation to obtain

$$\begin{aligned}b(r,z)=&-q(r,z)+\frac{z^2\mathsf{C1}'(r)}{2r}+\mathsf{C2}(r)+\frac{27\sigma(\sigma+z)}{64r^4}+\frac{7\pi\sigma}{128r^3}\\&-\frac{3r^2\left(r^2+\sigma(\sigma+2z)\right)}{4\left(r^2+(\sigma+z)^2\right)^3}+\frac{64r^2+4\sigma(4\sigma+15z)}{64\left(r^2+(\sigma+z)^2\right)^2}\\&+\frac{\sigma(\sigma-8z)}{32r^2\left(r^2+(\sigma+z)^2\right)}+\left(\frac{27\sigma(z-\sigma)(\sigma+z)}{64r^5}-\frac{7\sigma}{64r^3}\right)\tan^{-1}\left(\frac{\sigma+z}{r}\right),\end{aligned} \tag{92}$$

where $q(r,z)=g(r,z)+c(r,z)$, $C1(r)$ and $C2(r)$ are integration constants.

The rz equation is

$$\begin{aligned}&\frac{1}{64}\left(\frac{27\sigma}{r^4}-\frac{96r^2\sigma}{\left(r^2+(\sigma+z)^2\right)^3}+\frac{60\sigma}{\left(r^2+(\sigma+z)^2\right)^2}-\frac{4\sigma(\sigma-8z)(\sigma+z)}{r^2\left(r^2+(\sigma+z)^2\right)^2}\right.\\&\frac{768r^2z(\sigma+z)\left(r^2(\sigma+2z)-(z-\sigma)(\sigma+z)^2\right)}{\left(r^2+(\sigma+z)^2\right)^5}-\frac{16\sigma}{r^2\left(r^2+(\sigma+z)^2\right)}\\&+\frac{288r^2(\sigma+z)\left(r^2+\sigma(\sigma+2z)\right)}{\left(r^2+(\sigma+z)^2\right)^4}-\frac{16(\sigma+z)\left(16r^2+\sigma(4\sigma+15z)\right)}{\left(r^2+(\sigma+z)^2\right)^3}\\&\left.\frac{54\sigma z\tan^{-1}\left(\frac{\sigma+z}{r}\right)}{r^5}+\frac{27\sigma\left(z^2-\sigma^2\right)-7r^2\sigma}{r^4\left(r^2+(\sigma+z)^2\right)}\right)\\&-c^{(0,1)}(r,z)-q^{(0,1)}(r,z)-rq^{(1,1)}(r,z)+\frac{z\mathsf{C1}'(r)}{r}=0.\end{aligned} \tag{93}$$

This only involves first derivatives in z so we can integrate it to get

$$c(r,z) = \frac{27\sigma(\sigma+z)}{64r^4} + \frac{43\pi\sigma}{128r^3} + \frac{64r^2+\sigma(9z-2\sigma)}{16\left(r^2+(\sigma+z)^2\right)^2} \tag{94}$$

$$-\frac{r^2\left(35r^2+\sigma(17\sigma+36z)\right)}{4\left(r^2+(\sigma+z)^2\right)^3} - \frac{\sigma(17\sigma+26z)}{32r^2\left(r^2+(\sigma+z)^2\right)} + \frac{9r^4\left(r^2+\sigma(\sigma+2z)\right)}{2\left(r^2+(\sigma+z)^2\right)^4}$$
$$+\left(\frac{27\sigma(z-\sigma)(\sigma+z)}{64r^5} - \frac{43\sigma}{64r^3}\right)\tan^{-1}\left(\frac{\sigma+z}{r}\right)$$
$$-rq^{(1,0)}(r,z) - q(r,z) + \frac{z^2\mathsf{C1}'(r)}{2r} + \mathsf{C3}(r).$$

We are left with three more equations to solve: tt, rr and $\phi\phi$. Summing all three we arrive at

$$2r\mathsf{C1}'(r) + r\mathsf{C2}'(r) - r\mathsf{C3}'(r) + \frac{27\pi\sigma}{32r^3} = 0. \tag{95}$$

So, $C2(r) = -2\mathsf{C1}(r) + \mathsf{C3}(r) + \kappa_0 + \frac{9\pi\sigma}{32r^3}$. After this, all three equations are equivalent among themselves, so we just need to solve

$$\frac{1}{128r^7\left(r^2+(\sigma+z)^2\right)^4}\left(r\left(-64r^{10}+129\pi r^9\sigma+516\pi r^7\sigma(\sigma+z)^2\right.\right.$$
$$+774\pi r^5\sigma(\sigma+z)^4+516\pi r^3\sigma(\sigma+z)^6+129\pi r\sigma(\sigma+z)^8$$
$$12r^2\sigma(40\sigma+61z)(\sigma+z)^6+54\sigma(3\sigma+5z)(\sigma+z)^8$$
$$r^8\left(-462\sigma^2+384z^2-254\sigma z\right)+4r^4\sigma(\sigma+z)^4(83\sigma+92z)$$
$$\left.-4r^6(\sigma+z)^2\left(96\sigma^2+320z^2+343\sigma z\right)\right)$$
$$\left.-6\sigma\left(r^2+(\sigma+z)^2\right)^4\left(43r^2+45\left(\sigma^2-z^2\right)\right)\tan^{-1}\left(\frac{\sigma+z}{r}\right)\right)$$
$$-\frac{z^2\mathsf{C1}''(r)}{2r^2} + +\frac{z^2\mathsf{C1}'(r)}{2r^3} - \frac{\mathsf{C3}'(r)}{r}$$
$$-\frac{2q^{(0,1)}(r,z)}{z} + q^{(0,2)}(r,z) + \frac{3q^{(1,0)}(r,z)}{r} + q^{(2,0)}(r,z) = 0, \tag{96}$$

using the unknowns $C1(r)$, $C3(r)$, κ_0 and $q(r,z)$. We further redefine

$$\mathsf{C1}(r) = r\left(r\lambda\mathsf{0}''(r) + 3\lambda\mathsf{0}'(r)\right), \tag{97}$$

$$\mathsf{C3}(r) = r\lambda\mathsf{1}'(r) + 2\lambda\mathsf{1}(r), \tag{98}$$

$$q(r,z) = w(r,z) + \frac{z^2\mathsf{C1}(r)}{2r^2} + \lambda\mathsf{0}(r) + \lambda\mathsf{1}(r). \tag{99}$$

. This way only $w(r,z)$ enters the equation

$$\begin{aligned}
&-\frac{2w^{(0,1)}(r,z)}{z} + \frac{1}{128r^7\left(r^2+(\sigma+z)^2\right)^4}\Big(r\Big(-64r^{10}\\
&+129\pi r^9\sigma + 516\pi r^7\sigma(\sigma+z)^2 + 774\pi r^5\sigma(\sigma+z)^4\\
&+516\pi r^3\sigma(\sigma+z)^6 + 129\pi r\sigma(\sigma+z)^8 + 54\sigma(3\sigma+5z)(\sigma+z)^8\\
&4r^4\sigma(83\sigma+92z)(\sigma+z)^4 + 12r^2\sigma(40\sigma+61z)(\sigma+z)^6\\
&+r^8\left(-462\sigma^2+384z^2-254\sigma z\right) - 4r^6(\sigma+z)^2\left(96\sigma^2+320z^2+343\sigma z\right)\Big)\\
&-6\sigma\left(r^2+(\sigma+z)^2\right)^4\left(43r^2+45\left(\sigma^2-z^2\right)\right)\tan^{-1}\left(\frac{\sigma+z}{r}\right)\\
&+128r^6\left(r^2+(\sigma+z)^2\right)^4\left(3w^{(1,0)}(r,z) + r\left(w^{(0,2)}(r,z)+w^{(2,0)}(r,z)\right)\right)\Big) = 0.
\end{aligned} \tag{100}$$

Another redefinition,

$$w(r,z) = \frac{\mathsf{qt}^{(1,0)}(r,z) - z\mathsf{qt}^{(1,1)}(r,z)}{r}. \tag{101}$$

This simplifies the equation, allowing us to express the terms in $w(r,z)$ as a crossed derivative. Integrating with respect to r and z

$$\begin{aligned}
&\mathsf{qt}^{(2,0)}(r,z) + \mathsf{qt}^{(0,2)}(r,z) + \frac{\mathsf{qt}^{(1,0)}(r,z)}{r} - \frac{1}{256}\Bigg(\frac{4(15\pi z-34r)}{r^3}
\end{aligned} \tag{102}$$

$$\begin{aligned}
&\frac{54\sigma^2(2r+\pi z)}{r^5} + +\frac{\sigma(86\pi r+27z)}{r^4} + \frac{8\left(2z(\sigma+z)-3r^2\right)}{r^2\left(r^2+(\sigma+z)^2\right)} + \frac{48\left(2r^2-z(\sigma+z)\right)}{\left(r^2+(\sigma+z)^2\right)^2}\\
&-\frac{4\left(r^2(43\sigma+30z)+27\sigma(\sigma+z)^2\right)\tan^{-1}\left(\frac{\sigma+z}{r}\right)}{r^5}\Bigg) + zv(r,z) = 0,
\end{aligned}$$

where $v(r,z)$ is an unknown function with null cross derivative. We now try to write qt as a linear combination of stuff that appears in the equation, like $\arctan$,

inverse powers of r and so forth. We succeed in doing so and obtain that qt equals

$$\begin{aligned}\frac{1}{1024r^3\left(r^2+(\sigma+z)^2\right)}&(8\pi\left(r^2+(\sigma+z)^2\right)\left(r^2(43\sigma+30z)+3\sigma^2z\right)\\&+3r\left(r^2\left(56\sigma^2+32z^2+61\sigma z\right)+\sigma(\sigma+z)^2(56\sigma+29z)\right))\\&-\frac{\left(r^2(37\sigma+30z)+3\sigma(\sigma+z)^2\right)\tan^{-1}\left(\frac{\sigma+z}{r}\right)}{64r^3}\\&+\frac{1}{4}\log\left(r^2+(\sigma+z)^2\right).\end{aligned}\tag{103}$$

Note we still have freedom in redefining $qt(r,z)\to qt(r,z)+\hat{q}(r,z)$,where $\hat{q}(r,z)$ satisfies

$$\hat{q}^{(0,2)}(r,z)+\frac{\hat{q}^{(1,0)}(r,z)}{r}+\hat{q}^{(2,0)}(r,z)+zv(r,z)=0\tag{104}$$

and v is an unknown function whose cross derivative is null. This solves the Einstein equations.

Boundary Conditions

We still have the free parameters κ_0, $\lambda_0(r)$, $\lambda_1(r)$, $\hat{q}(r,z)$ and $v(r,z)$. We need to fix them to make sure that spacetime is asymptotically AdS, that is

$$g(r,z=0)=b(r,z=0)=c(r,z=0)=0.\tag{105}$$

We define $\beta(r) = \lambda_1(r) - \lambda_0(r)$. With a few manipulations, the conditions (105) become

$$\frac{8r^5 + 5r^3\sigma^2 + 3\sigma\left(r^2+\sigma^2\right)^2 \tan^{-1}\left(\frac{\sigma}{r}\right) + 3r\sigma^4}{32r^2\left(r^2+\sigma^2\right)^2} \tag{106}$$
$$+r\hat{q}^{(2,0)}(r,0) + \hat{q}^{(1,0)}(r,0) + r^2\lambda\mathsf{0}'(r) + 2r\lambda\mathsf{0}(r) = 0,$$
$$\frac{1}{64r^4\left(r^2+\sigma^2\right)}\left(r\left(64\kappa\mathsf{0}r^6 + 43\pi r^3\sigma\ + 13r^2\sigma^2 + 43\pi r\sigma^3\right.\right.$$
$$\left.\left.16r^4\left(4\kappa\mathsf{0}\sigma^2 - 1\right) + 45\sigma^4\right) - 4\sigma\left(r^2+\sigma^2\right)\left(11r^2+9\sigma^2\right)\tan^{-1}\left(\frac{\sigma}{r}\right)\right)$$
$$-\hat{q}^{(1,0)}(r,0) - 2r^3\lambda\mathsf{0}''(r) + r^2\beta'(r) - 5r^2\lambda\mathsf{0}'(r) + r\beta(r) = 0,$$
$$\frac{1}{128r^5\left(r^2+\sigma^2\right)^2}(r\left(32r^6 - 43\pi r^5\sigma + 76r^4\sigma^2\ - 86\pi r^3\sigma^3 - 16r^2\sigma^4\right.$$
$$\left.-43\pi r\sigma^5 - 36\sigma^6\right) + 2\sigma\left(r^2+\sigma^2\right)^2\left(31r^2+9\sigma^2\right)\tan^{-1}\left(\frac{\sigma}{r}\right))$$
$$-\hat{q}^{(2,0)}(r,0) + \beta(r) - r\lambda\mathsf{0}'(r) = 0. \tag{107}$$

We now try to integrate these equations. For example, in the first equation, notice that

$$\frac{\partial\left(r\hat{q}^{(1,0)}(r,0) + r^2\lambda\mathsf{0}(r)\right)}{\partial r} = r\hat{q}^{(2,0)}(r,0) + \hat{q}^{(1,0)}(r,0) + r^2\lambda\mathsf{0}'(r) + 2r\lambda\mathsf{0}(r) \tag{108}$$

and so it is readily integrable. Proceeding in such a manner, we eventually arrive at

$$\hat{q}(r,0) = c_1 r^2 + \frac{1}{64}\left(-8A + 16F + 3\log\left(r^2+\sigma^2\right) - \log(r) - 2\right. \tag{109}$$
$$\left.\left(-16A + 32B + 8\kappa\mathsf{0}r^2 + 4\log\left(r^2+\sigma^2\right) - 4\log\left(\frac{r^2}{\sigma^2}+1\right) + 10\right) + 2\mathsf{Li}_2\left(-\frac{r^2}{\sigma^2}\right)\right), \tag{110}$$

$$\beta(r) = \frac{1}{128r^5\left(r^2+\sigma^2\right)}\left(r\left(8r^4\left(4A + 24B - 2\kappa\mathsf{0}r^2 - 9\right) + 43\pi r^3\sigma + 4r^2\right.\right. \tag{111}$$
$$\left.\sigma^2\left(8A + 48B - 4\kappa\mathsf{0}r^2 - 7\right) + 43\pi r\sigma^3 + 36\sigma^4\right) + 2\left(r^2+\sigma^2\right)$$
$$\left.16r^5\left(8c_1 - \kappa\mathsf{0}\log(r)\right) - \left(49r^2\sigma + 9\sigma^3\right)\tan^{-1}\left(\frac{\sigma}{r}\right) + 12r^3\log\left(r^2+\sigma^2\right)\right),$$

$$\lambda_0(r) = \frac{2r\left(-4A - 8B + 2r^2\left(\kappa 0 - 16c_1\right) + 4\kappa 0 r^2 \log(r) - \log\left(r^2+\sigma^2\right) + 1\right) + 3\sigma \tan^{-1}\left(\frac{\sigma}{r}\right)}{32r^3}. \tag{112}$$

C - Weyl Tensor: definition and properties

[23]The Riemann tensor has three basic symmetries

- $R_{abcd} = -R_{bacd}$
- $R_{abcd} = -R_{abdc}$
- $R_{abcd} + R_{cabd} + R_{bcad} = 0$

Because of this, it has $D^2\frac{(D^2-1)}{12}$ independent components, instead of D^4. Because of the Bianchi identities and the fact that it is a symmetric tensor, the Ricci tensor has $\frac{D}{2}(D+1) - D = \frac{D}{2}(D-1)$ independent components. For example, for $D = 4$, the Riemann tensor has 20 independent components and the Ricci tensor only 6.

The point of defining the Weyl tensor is to have an object which has all the degrees of freedom contained in the Riemann tensor which are *not* contained in the Ricci tensor. It is defined as

$$W_{abcd} := R_{abcd} + \frac{2}{D-2}(g_{a[d}R_{c]b} - g_{b[d}R_{c]a}) - \frac{2}{(D-1)(D-2)}Rg_{a[d}g_{c]b} \tag{113}$$

It has the same three basic symmetry properties as the Riemann tensor. Also, it obeys $W^a_{bad} = 0$.

In our work, $W^2 := W^{abcd}W_{abcd}$ goes to a constant for large ϕ_B. We interpret this as having the Riemann tensor getting as constant as it can, while the Ricci tensor still simultaneously solves the Einstein equations.

D - Spectral method: Numerical Hurdles

The procedure we outlined to solve the Einstein equations involves writing a matrix G. Since our equations involve six unknowns, the matrix G has $6^2 \times$

[23]We follow [11] here.

$N_x^2 \times N_y^2$ entries, where N_x is the number of nodes in the x direction and N_y is the number of nodes in the y direction. Now suppose we want to use a grid 200×200. In that case the matrix has 5.76×10^{10} elements. If we use a programming language that uses 8 bytes to store each entry (which is typical), then that matrix occupies 460 Gb of memory!

A way to overcome this problem is to take advantage of the structure that the matrix G has. Let us see that in an example. Consider a PDE in two dimensions x and y for the variable q,

$$\frac{\partial^2 q}{\partial x^2} + \frac{\partial^2 q}{\partial y^2} + q^2 \frac{\partial q}{\partial x} = 0. \tag{114}$$

After discretizing, we get a set f_{ij} of nonlinear equations,

$$\sum_m (Difxx)_{jm} q_{im} + (Difyy)_{im} q_{mj} + q_{ij}^2 (Difx)_{jm} q_{im} = 0, \tag{115}$$

where the matrix $Difx$ is a differentiation matrix in the x direction, $Dify$ is a differentiation matrix in the y direction, $Difxx$ is a second derivative differentiation matrix in the x direction and so on. The matrix $G_{ijkl} \equiv \frac{\partial f_{ij}}{\partial q_{kl}}$ is defined as

$$G_{ijkl} = \sum_m (Difxx)_{jl}\delta_{ik} + (Difyy)_{ik}\delta_{jl} + 2q_{ij}(Difx)_{jm} q_{im}\delta_{ik}\delta_{jl} + q_{ij}^2 (Difx)_{jl}\delta_{ik}. \tag{116}$$

It is clear that, for the general case of a second order PDE, we can always write G_{ijkl} as

$$\begin{aligned} G_{ijkl} = {} & (cx)_{ij}(Difx)_{jl}\delta_{ik} + (cxx)_{ij}(Difxx)_{jl}\delta_{ik} \\ & + (cy)_{ij}(Dify)_{ik}\delta_{jl} + (cyy)_{ij}(Difyy)_{ik}\delta_{jl} \\ & + (cxy)_{ij}(Dify)_{ik}(Difx)_{jl} + (cId)_{ij}\delta_{ik}\delta_{jl}, \end{aligned} \tag{117}$$

where $(cx)_{ij}$, $(cy)_{ij}$, $(cxx)_{ij}$, $(cyy)_{ij}$, $(cxy)_{ij}$ and $(cId)_{ij}$ are coefficients which can be obtained from our particular PDE[24]. In the example (116), $(cx)_{ij} = q_{ij}^2$, $(cy)_{ij} = 0$, $(cxx)_{ij} = 1$, $(cyy)_{ij} = 1$, $(cxy)_{ij} = 0$ and finally $(cId)_{ij} = \sum_m 2q_{ij}(Difx)_{jm} q_{im}$.

Notice that each coefficient has just $N_x \times N_y$ entries. For example, if use a 200×200 grid, storing these coefficients and the differentiation matrices only

[24] $(cId)_{ij}$ is the coefficient for the identity matrix.

occupies 1 Mb of memory. This should be contrasted with the value 460 Gb we encountered before. We think that in order to make further progress we must take into account this fact.

E - Spectral method: convergence properties

[25] We now illustrate some of the convergence properties of the spectral method we are using. We consider the calculation we did for the IR horizon. We can see in figure 18 how the norm of the deTurck vector behaves as we enlarge our grid.

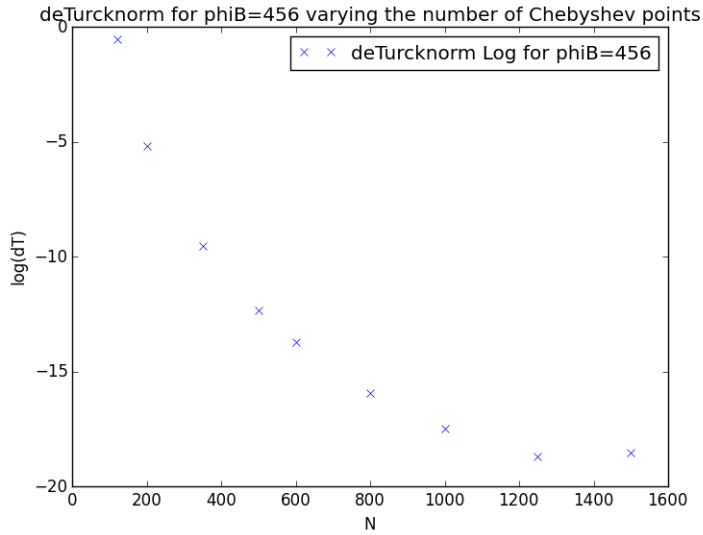

Figure 18: The logarithm is in base 10 (the same is true for the following graphs). For $N > 400$, the deTurck vector norm is below 10^{-10} which is the threshold we estabilished for the validity of our results.

In order for our numerical work to have significance, we must demand that the value of scalars for a certain ϕ_B converges if we use an increasingly large grid. The graphs 19 and 20 illustrate just that.

[25] The ideia for this section was motivated by the master's thesis [12].

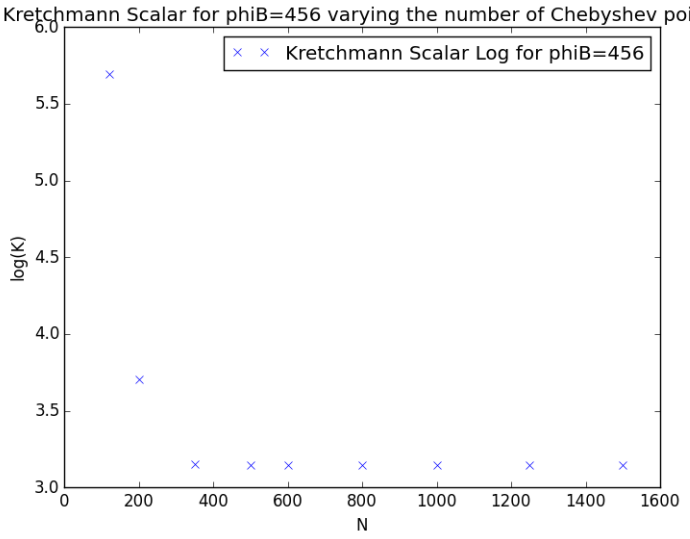

Figure 19: For $N > 400$, the maximum of the Kretchmann scalar converges to a fixed value.

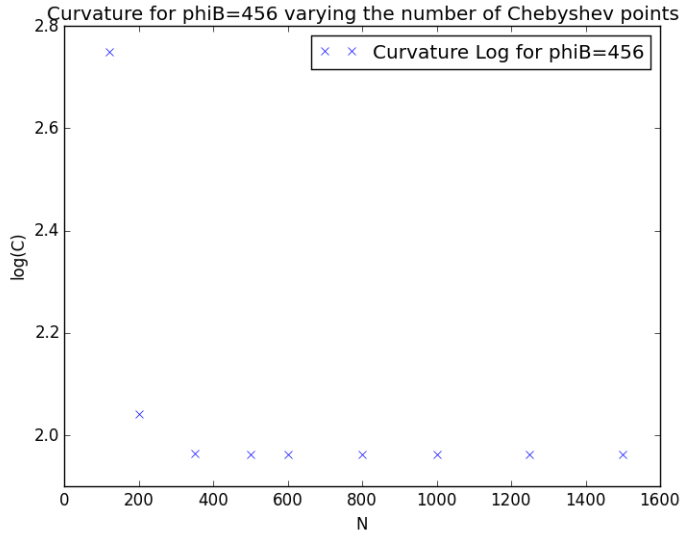

Figure 20: For $N > 400$, the maximum of the curvature converges to a fixed value.

F - Code Display

In order to give a flavour of the numerical calculations, we will display some important parts of our code.

```
while max(abs(delta))>10**(-10):
    v=f(u);G=H(u) #u is a vector that contains the metric unknowns q1, q2, ...
    delta=solve(G,-v) #v is the vector that represents the Einstein eqs at u
    u=delta+u #G is the matrix that enters Newton's method
```

Figure 21: Three line code implementing Newton's method. This part of the code is the same for PDE's and ODE's. We say that Newton's method converges when the changes it provokes to the metric unknowns are smaller than 10^{-10}.

```
PythUsual = {a[x] → a, b[x] → b, c[x] → c, d[x] → d, D[a[x], x] → 2 * dDifA, D[b[x], x] → 2 * dDifB,
   D[c[x], x] → 2 * dDifC, D[d[x], x] → 2 * dDifD, D[D[a[x], x], x] → 4 * dDif2A,
   D[D[b[x], x], x] → 4 * dDif2B, D[D[c[x], x], x] → 4 * dDif2C, D[D[d[x], x], x] → 4 * dDif2D};

eqsfinal1 are the Einstein equations.

eqspyth = eqsfinal1 /. PythUsual;

FortranForm[eqspyth[[4]]]

    (4 * b * c * dDifA * x * (2 - 3 * x ** 2 + x ** 4) * (2 * d * x + 2 * dDifD * (-1 + x ** 2)) +
-   a * (-16 * b ** 2 * c * d * x - 2 * c * dDifB * x * (2 - 3 * x ** 2 + x ** 4) * (2 * d * x + 2 * dDifD * (-1 + x ** 2)) +
-     b * (2 * dDifC * x * (2 - 3 * x ** 2 + x ** 4) * (2 * d * x + 2 * dDifD * (-1 + x ** 2)) +
-       2 * c * (8 * d * x + (-1 + x ** 2) ** 2 * (4 * dDif2D * x * (-2 + x ** 2) +
-  2 * dDifD * (-2 + 3 * x ** 2))))) / (2. * a * b * c * (-2 + x ** 2))
```

Figure 22: This figure shows how we pass equations from Mathematica to Python. *PythUsual* is a substitution rule that turns functions' names written in Mathematica language to the names of the corresponding arrays written in Python language. *FortranForm* also helps, as Fortran's syntax is not so different from Python's. The fourth component of $f(u)$ is displayed.

```
def cheb(N):
    #returns N+1 chebysev nodes and a N+1 times N+1 diff matrix
    xs=cos(pi*arange(0,N+1)/N)
    b=ones(N+1); b[0]=2; b[N]=2
    c=b*array([(-1)**i for i in range(0,N+1)])
    X=transpose(tile(xs,(N+1,1)))
    dX=X-transpose(X)
    D=outer(c,1./c)/(dX+eye(N+1))
    D=D-diag(sum(transpose(D),0))
    return xs, D

N=1000 #Number of Chebyshev points
xs,Difl=cheb(N) #Difl is the differentiation matrix

#a, b, c, and d represent the metric unknowns
#dDifA, dDifB, ... , are the derivatives of a, b, ...

dDifA=dot(Difl,a); dDifB=dot(Difl,b)
dDifC=dot(Difl,c); dDifD=dot(Difl,d)
```

Figure 23: *cheb(N)* gives the differentiation matrices. See [4] for the formulas.

```
Derivative with respect to the function a

eqsm = eqsfinal1 /. {a[x] → a , D[a[x], x] → f[a], D[D[a[x], x], x] → g[a]};
DerA = D[eqsm, a];
F = SeriesCoefficient[DerA /. {D[g[a], a] → Y^2, D[f[a], a] → Y}, {Y, 0, 0}];
PythonTs = {f[a] → 2 * dDifA, D[f[a], a] → 2 * Dif, g[a] → 4 * dDif2A,
   D[g[a], a] → 4 * Dif2, b[x] → b, c[x] → c, d[x] → d, D[b[x], x] → 2 * dDifB,
   D[c[x], x] → 2 * dDifC, D[d[x], x] → 2 * dDifD, D[D[b[x], x], x] → 4 * dDif2B,
   D[D[c[x], x], x] → 4 * dDif2C, D[D[d[x], x], x] → 4 * dDif2D};
DerA = (DerA - F + F * eye) /. PythonTs;
Clear[eqsm, F, PythonTs]
FortranForm[DerA[[3]]]

\Form=
      eye*((2*b*(4*c + 2*dDifC*x*(2 - 3*x**2 + x**4) +
     -          4*c**2*x**2*(-2 + x**2)*(3 + 2*d**2*(-1 + x**2)**2)) +
     -       (-1 + x**2)*(-8*c**2*(-1 + x**2) -
     -          4*dDifC**2*x**2*(-2 + x**2)**2*(-1 + x**2) +
     -          c*x**2*(-2 + x**2)*
     -           (2*dDifC*x*(-5 + 3*x**2) + 4*dDif2C*(2 - 3*x**2 + x**4))))/
     -     (a*c*(-2 + x**2)**2) -
     -    (-4*b*c*x**2*(-2 + x**2)*(4*c + 2*dDifC*x*(2 - 3*x**2 + x**4)) +
     -       a*(2*b*(4*c + 2*dDifC*x*(2 - 3*x**2 + x**4) +
     -             4*c**2*x**2*(-2 + x**2)*(3 + 2*d**2*(-1 + x**2)**2)) +
     -          (-1 + x**2)*(-8*c**2*(-1 + x**2) -
     -             4*dDifC**2*x**2*(-2 + x**2)**2*(-1 + x**2) +
     -             c*x**2*(-2 + x**2)*
     -              (2*dDifC*x*(-5 + 3*x**2) + 4*dDif2C*(2 - 3*x**2 + x**4)))))/
     -     (a**2*c*(-2 + x**2)**2))
```

Figure 24: Writing the matrix G that enters Newton's method in Mathematica. The code above gets Mathematica to compute functional derivatives.

References

[1] G. T. Horowitz, N. Iqbal, J. E. Santos, and B. Way, "Hovering Black Holes from Charged Defects," *Class. Quant. Grav.*, vol. 32, no. 10, p. 105001, 2015.

[2] T. Wiseman, *Numerical construction of static and stationary black holes*. 2011.

[3] P. Figueras, J. Lucietti, and T. Wiseman, "Ricci solitons, Ricci flow, and strongly coupled CFT in the Schwarzschild Unruh or Boulware vacua," *Class. Quant. Grav.*, vol. 28, p. 215018, 2011.

[4] L. Trefethen, *Spectral Methods in Matlab*. 2000.

[5] L. P. Eisenhart, *Riemannian Geometry*. Princeton University Press, 1949.

[6] J. I. Kapusta, *Finite Temperature Field Theory*, vol. 360 of *Cambridge Monographs on Mathematical Physics*. Cambridge: Cambridge University Press, 1989.

[7] J. McGreevy, "Holographic duality with a view toward many-body physics," *Adv. High Energy Phys.*, vol. 2010, p. 723105, 2010.

[8] K. Skenderis, "Lecture notes on holographic renormalization," *Class. Quant. Grav.*, vol. 19, pp. 5849–5876, 2002.

[9] S. A. Hartnoll, C. P. Herzog, and G. T. Horowitz, "Holographic Superconductors," *JHEP*, vol. 12, p. 015, 2008.

[10] S. A. Hartnoll, C. P. Herzog, and G. T. Horowitz, "Building a Holographic Superconductor," *Phys. Rev. Lett.*, vol. 101, p. 031601, 2008.

[11] S. W. Hawking and G. F. R. Ellis, *The Large Scale Structure of Space-Time*. Cambridge Monographs on Mathematical Physics, Cambridge University Press, 2011.

[12] M. Oliveira, *Spectral methods in general relativity: polarized black holes in AdS space.* 2013.